

RESEARCH PAPER



Drug-like molecules with anti-trypanothione synthetase activity identified by high throughput screening

Diego Benítez^a, Jaime Franco^{a*}, Florencia Sardi^{a†}, Alejandro Leyva^b, Rosario Durán^b, Gahee Choi^{d‡}, Gyongseon Yang^{d§}, Taehee Kim^{c¶}, Namyoul Kim^{c&}, Jinyeong Heo^c, Kideok Kim^e, Honggun Lee^e, Inhee Choi^f, Constantin Radu^{e**}, David Shum^c, Joo Hwan No^d and Marcelo A. Comini^a

^aLaboratory Redox Biology of Trypanosomes, Institut Pasteur de Montevideo, Montevideo, Uruguay; ^bAnalytical Biochemistry and Proteomics Unit, Institut Pasteur de Montevideo, Instituto de Investigaciones Biológicas Clemente Estable, Montevideo, Uruguay; ^cAssay Development and Screening, Institut Pasteur Korea, Gyeonggi-do, Republic of Korea; ^dHost-Parasite Research Laboratory, Institut Pasteur Korea, Gyeonggi-do, Republic of Korea; ^eAutomation and Logistics Management, Institut Pasteur Korea, Gyeonggi-do, Republic of Korea; ^fMedicinal Chemistry, Institut Pasteur Korea, Gyeonggi-do, Republic of Korea

ABSTRACT

Trypanothione synthetase (TryS) catalyses the synthesis of *N*¹,*N*⁸-bis(glutathionyl)spermidine (trypanothione), which is the main low molecular mass thiol supporting several redox functions in trypanosomatids. TryS attracts attention as molecular target for drug development against pathogens causing severe and fatal diseases in mammals. A drug discovery campaign aimed to identify and characterise new inhibitors of TryS with promising biological activity was conducted. A large compound library (*n* = 51,624), most of them bearing drug-like properties, was primarily screened against TryS from *Trypanosoma brucei* (*TbTryS*). With a true-hit rate of 0.056%, several of the *TbTryS* hits (IC₅₀ from 1.2 to 36 μM) also targeted the homologue enzyme from *Leishmania infantum* and *Trypanosoma cruzi* (IC₅₀ values from 2.6 to 40 μM). Calmidazolium chloride and Ebselen stand out for their multi-species anti-TryS activity at low μM concentrations (IC₅₀ from 2.6 to 13.8 μM). The moieties carboxy piperidine amide and amide methyl thiazole phenyl were identified as novel *TbTryS* inhibitor scaffolds. Several of the TryS hits presented one-digit μM EC₅₀ against *T. cruzi* and *L. donovani* amastigotes but proved cytotoxic against the human osteosarcoma and macrophage host cells (selectivity index ≤ 3). In contrast, seven hits showed a significantly higher selectivity against *T. b. brucei* (selectivity index from 11 to 182). Non-invasive redox assays confirmed that Ebselen, a multi-TryS inhibitor, induces an intracellular oxidative milieu in bloodstream *T. b. brucei*. Kinetic and mass spectrometry analysis revealed that Ebselen is a slow-binding inhibitor that modifies irreversible a highly conserved cysteine residue from the TryS's synthetase domain. The most potent *TbTryS* inhibitor (a singleton containing an adamantane moiety) exerted a non-covalent, non-competitive (with any of the substrates) inhibition of the enzyme. These data feed the drug discovery pipeline for trypanosomatids with novel and valuable information on chemical entities with drug potential.

ARTICLE HISTORY

Received 19 October 2021
Revised 2 February 2022
Accepted 18 February 2022

KEYWORDS



Trypanothione synthetase; *Leishmania*; *Trypanosoma*; covalent inhibitor; non-competitive inhibition

Introduction

Diseases caused by trypanosomatids (e.g. Leishmaniasis, Chagas disease and African sleeping sickness) represent a major health problem in endemic regions and an emerging threat in industrialised countries due to global migration. To date, the therapeutic arsenal to combat human Trypanosomiasis and Leishmaniasis is rather limited in quantity and quality (low efficacy, safety, high cost and difficult administration) as it is also the number of backup drugs that await (pre)clinical assessment¹.

Devoid of catalase and canonical thioredoxin- and glutaredoxin-redox systems, the thiol-redox homeostasis of trypanosomatids

depends exclusively on a molecule absent in mammals: the polyamine dithiol *N*¹,*N*⁸-bis(glutathionyl)spermidine or trypanothione² (T(SH)₂, Figure 1). Trypanothione biosynthesis is carried out by a bifunctional enzyme, namely trypanothione synthetase (TryS), harbouring an N-terminal amidase domain homologous to the catalytic domain of papain-like cysteine peptidases³ that is fused to an ATP-dependent carbon-nitrogen ligase domain homologous to the ATP-grasp superfamily of enzymes⁴. A paralog enzyme, namely monoglutathionylspermidine amidase/synthetase (GspS), with capacity to synthesise the conjugation of only one molecule of glutathione (GSH) to the polyamine moiety, is expressed by some

CONTACT Marcelo A. Comini  mcomini@pasteur.edu.uy  Laboratory Redox Biology of Trypanosomes, Institut Pasteur de Montevideo, Matajojo 2020, Montevideo 11400, Uruguay

*Present address: Chemistry for Nucleic Acid Recognition UMR9187/U1196, Institut Curie. 110 Rue Henri Becquerel, Orsay 91400, France.

**Molecular Devices, 3860 N First Street, San Jose, CA 95134, USA.


†Present address: Virbac S.A, Avenida Millán 4175, Montevideo 12900, Uruguay.

‡Present address: Discovery team, Discovery unit, Research and Early Development, GC Pharma, Yongin-si, Gyeonggi-do 16924, Republic of Korea.

§Present address: Merck Sharp/Dohme, Korea Ltd, Seoul 04637, Republic of Korea.

¶Present address: Mogam Institute for Biomedical Research, Yongin-si, Gyeonggi-do 16924, Republic of Korea.

&Present address: TwinpigBiolab Inc., Dongdaemun-gu, Seoul 02453, Republic of Korea.

 Supplemental data for this article can be accessed [here](#).

© 2022 The Author(s). Published by Informa UK Limited, trading as Taylor & Francis Group.

This is an Open Access article distributed under the terms of the Creative Commons Attribution-NonCommercial License (<http://creativecommons.org/licenses/by-nc/4.0/>), which permits unrestricted non-commercial use, distribution, and reproduction in any medium, provided the original work is properly cited.

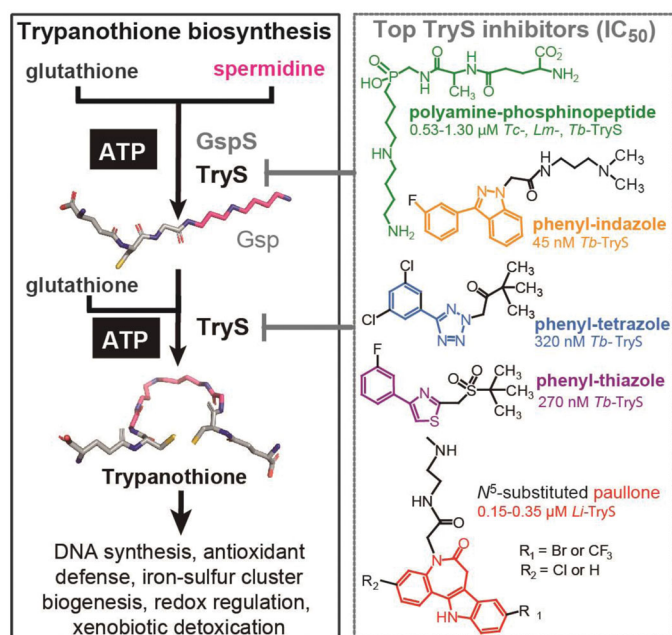


Figure 1. Trypanothione biosynthesis/functions and inhibitors. Trypanothione synthetase (TryS) catalyses the stepwise addition of one or two glutathione molecules to spermidine or monoglutathionylspermidine (Gsp) to form trypanothione. In contrast, monoglutathionylspermidine synthetase (GspS) is able to add a single glutathione molecule to spermidine to form monoglutathionylspermidine (Gsp). The biosynthetic reactions are ATP-dependent. The structure and IC_{50} value of the most potent TryS inhibitors (*Tc*: *T. cruzi*, *Lm*: *L. major*, *Tb*: *T. brucei* and *Li*: *L. infantum*) emerging from a large (phenyl-indazole, -tetrazole and -thiazole) or drug-focused (polyamine-phosphinopeptide and paullone) screenings are shown.

trypanosomatids⁵. TryS is indispensable for parasite survival since GSH cannot take over T(SH)₂ functions⁵⁻⁹, in part, because many enzymes with thiol-active groups evolved specificity for using bis-glutathionyl spermidine as redox substrate¹⁰. In line with experimental evidences from dsRNA^{5,11} and/or chemical inhibition approaches^{8,9,11-13} that lead to partial suppression of TryS activity, this enzyme has been shown to be one of the bottle-necks for the metabolic output of the trypanothione pathway¹⁴. Thus, at variance with other components of this pathway, even partial inhibition of TryS impairs parasite survival *in vivo*¹¹ and increase pathogen's susceptibility to most clinical drugs^{7,9}.

The search and development of TryS inhibitors was initially biased towards substrate-like and mechanism-based molecules¹⁵⁻²². Despite their reasonable anti-TryS activity *in vitro* (e.g. nanomolar IC_{50}), the majority of the compounds failed to exert anti-proliferative activity against pathogenic trypanosomatids, probably due to their peptidic nature that make them prone to hydrolysis by esterases and amidases²³.

Up to date, there is a single report for a large HTS against TryS¹². The study involved a library of nearly 62,000 compounds and *Tb*TryS as molecular target. Pharmacophore structures (Figure 1) with nM potency against the enzyme (IC_{50} 95–317 nM) and 36- to 99-fold higher EC_{50} against bloodstream *T. brucei* (EC_{50} 5–10 μM) were identified and the on-target effect was confirmed for the compound with highest anti-*T. brucei* activity (phenyl-indazole, Figure 1).

Although some physicochemical properties (low MW, Log *P* < 5 and low polar surface area) of the candidate scaffolds were improved by a hit-to-lead optimisation campaign, none of the new molecules superseded the anti-*T. brucei* or anti-TryS activity of the original ones^{12,24}. Furthermore, none of these compounds were tested for their potential broad range activity against other

TryS and trypanosomatid species neither for their pharmacological performance in animal infection models.

With the aim to identify multi-TryS inhibitors, we recently reported the establishment of a 96-well plate HTS assay against TryS from the three major trypanosomatid species (*Trypanosoma cruzi*: *Tc*, *Leishmania infantum*: *Li*, and *Trypanosoma brucei*: *Tb*)²⁵. From a small but chemically diverse compound library (*n* = 144), several hits with TryS species-specific activity were identified. The most potent compounds targeted *Li*TryS and belonged to the scaffold N^5 -acetamide substituted, 3-chlorokenpaullone (Figure 1). A series of analogues containing different substituents at position N^5 of the 3-chlorokenpaullone were synthesised and yielded TryS hits that gained activity against the *T. cruzi* enzyme and infective stage of the parasite^{9,26} or showed improved selectivity for the intracellular form of *L. infantum*¹³. In both cases, the new analogues retained their on-target effect against the pathogen as confirmed by genetic⁹ or metabolic approaches¹³. Kinetic, thermodynamic and computational approaches suggested that paullones occupy the polyamine and second glutathione binding site of TryS¹³. Yet, the identification of multi-spectrum TryS inhibitors with reasonable biological activity and selectivity proved unsuccessful.

One of the major factors contributing to failure during the early phase of the drug discovery process is ascribed to the poor drug-like properties of the hits or to the impossibility to attain it during optimisation. This is particularly challenging for diseases caused by trypanosomatids since each species show different tropism and clinical manifestations (i.e. haemolympathic, meningoencephalic, muco-cutaneous, visceral), which may demand disease-specific drugs/formulations to achieve a proper biodistribution.

In order to pave the way towards the identification of new molecules inhibiting TryS and/or the proliferation of the infective stages of biomedically relevant trypanosomatids, we performed a target-based HTS of a large and diverse chemolibrary.

*Tb*TryS was selected as molecular target because it has the lowest K_M values for substrates²⁵ and, therefore, represents a challenging molecular target for finding potent and selective inhibitors with wide-spectrum activity. The screening assay was adapted to favour the detection of non-competitive and slow-binding inhibitors, in addition to potent competitive ones. The *Tb*TryS hits were further tested for their capacity to inhibit TryS from *T. cruzi* and *L. infantum*, and those displaying satisfactory inhibition against the molecular target were screened for their anti-trypanosomatid and host-cell cytotoxicity. The inhibition mechanism for non-competitive TryS inhibitors was elucidated. In conclusion, this study disclosed a set of novel compounds with potential to be optimised as TryS or anti-trypanosomal inhibitors.

Materials and methods

Reagents

Unless otherwise stated all chemical reagents were of analytical grade and purchased from Sigma-Aldrich (St. Louis, MO). The libraries or single compounds employed in the pilot and large HTS, or subsequent studies, respectively, were purchased to LOPAC® (SIGMA), Selleck Chemicals, NIH clinical, TOCRIS and ENAMINE. Human acute monocytic leukaemia cell line THP-1 (TIB-20™), human osteosarcoma cell line U-2 OS (HTB-96™) and rhesus monkey kidney epithelial cell LLC-MK2 (CCL-7™) were purchased from the ATCC®.

Heterologous expression and purification of recombinant TryS

Expression and purification of His-tagged *TcTryS*, *LiTryS* and *TbTryS* were performed according to protocols previously reported²⁵ except that the size exclusion chromatography (SEC) was performed with a HiLoad®16/60 Superdex®200 pg column (GE Healthcare, Chicago, IL). This column was equilibrated in running buffer (10 mM MgSO₄, 0.5 mM EDTA, 100 mM HEPES pH 7.4, containing DTT 1 mM and 150 mM NaCl) and injected with 2 ml of a TryS sample (≤60 mg/mL protein) from the peak of the preceding chromatographic step. SEC was performed at a flow rate of 0.75 ml/min, at 4 °C using an Äkta-FPLC device (GE Healthcare). About 6 mg and 30 mg TryS per litre of culture medium were obtained for *TcTryS* and *LiTryS* or *TbTryS*, respectively. The purity and specific activity of the recombinant TryS, assessed by SDS-PAGE and enzymatic assays, resembled those reported earlier²⁵. The recombinant enzymes (6–10 mg/mL TryS in running buffer containing 40% v/v glycerol) were stored at –20 °C until use.

High-throughput TryS assay

General considerations

The TryS assay consists in quantifying the inorganic phosphate (Pi), released from ATP during catalysis, which is detected upon complexation to the colorimetric reagent BIOMOL GREEN™ (Enzo Life Sciences, Farmingdale, NY). The original screening assay (96-well plate and reaction volume = 50 µL)²⁵ was miniaturised to a 384-well plate and a total reaction volume of 16 µL. The assay conditions were adjusted to yield optimal signal (absorbance ≤ 0.6) and to increase the chances to detect slow-binding as well as potent competitive inhibitors. Hence, substrates were added at near-physiological concentrations (≥ *K_M* values) that do not interfere with the colorimetric reaction [ATP 150 µM, spermidine (SP) 2 mM and glutathione (GSH) 150 µM] and compounds were pre-incubated for 1 h with TryS before starting the reaction. Under these conditions, the limit of detection (LOD; calculated as the Pi concentration corresponding to three SD of the blank mean *A*_{620 nm}) and the sensitivity (slope for *A*_{620 nm} versus Pi concentration) of the screening assay was ~0.9 µM Pi and ~0.008 (*R*² ~0.98), respectively (Figure S1(A)). The reaction was stopped by chelating Mg⁺⁺ with EDTA (end concentration 50 mM). The concentration-dependent effect of EDTA in assay sensitivity and signal stability is shown in Figure S1(B,C).

The compounds were tested at a final concentration of 25 µM and, whenever possible, from freshly prepared solutions. All procedures were performed at room temperature (RT, 23–26 °C) and false positive hits were discriminated in subsequent tests (Dose response curves, DRC and interference assays). Assay automation was achieved using a Personal Pipettor liquid handler (Apricot Designs, Covinba, CA), a Matrix Wellmate Microplate Dispenser (Thermo Fisher Scientific, Waltham, MA), a Multidrop™ Combi Reagent Dispenser (Thermo Fisher Scientific), a robotic arm Plate Handler II and an Envision multilabel reader (both from Perkin Elmer, Waltham, MA). Full details of the standard operating procedure (SOP) used for the HTS assay are provided as Supplemental materials.

TryS inhibition is expressed as follows: % Inhibition = $\frac{\{(A_{620\text{ nm}}\text{ C-} - A_{620\text{ nm}}\text{ C+}) - (A_{620\text{ nm}}\text{ Cx} - A_{620\text{ nm}}\text{ C+})\}}{(A_{620\text{ nm}}\text{ C-} - A_{620\text{ nm}}\text{ C+})} \times 100$, where *A*_{620 nm} Cx is the mean absorbance at 620 nm for the reaction test with compound *x* at 25 µM, *A*_{620 nm} C+ is the mean absorbance at 620 nm for the “inhibition control” with DMSO and reaction buffer, *A*_{620 nm} C- is the mean absorbance at 620 nm for the “activity control” with DMSO and enzyme. Error

values, which never exceeded 10%, are expressed as percentage calculated as follows: $(\sigma^{n-1}/C-) \times 100\%$, where σ^{n-1} refers to one standard deviation (SD).

Hits' validation

All *TbTryS* hits were repurchased and retested at 25 µM against the *T. brucei* enzyme, as well as again *TcTryS* and *LiTryS*. Enzyme concentration was adjusted for each TryS (*TbTryS* = 6.1×10^{-6} µmol/min mL, *TcTryS* = 2.1×10^{-6} µmol/min mL and *LiTryS* = 6.5×10^{-6} µmol/min mL) to obtain a satisfactory linear regression for *A*_{620 nm} versus time under the assay conditions (Figure S1(D–F)). For each TryS, the substrates' concentrations used in the assay are the same reported previously²⁵.

The screening at 25 µM was performed in a 384-well plate, essentially as described in the previous section, except for: (a) the compounds were evaluated by quadruplicate, (b) the reagents were dispensed manually using a 16-multichannel pipette (Thermo Fisher Scientific Finnpiptette), (c) the reaction was performed at controlled temperature (28 °C) and stopped by addition of the BIOMOL GREEN™ reagent, and (d) absorbance at 620 nm was measured with a MultiScan FC plate reader (Thermo Fisher Scientific).

The compounds showing TryS inhibition ≥ 50% at 25 µM were subjected to DRC studies, performed at eight-point concentrations starting from 125 µM and 1:3 serial dilutions. In all assays, the DMSO concentration was 1.25% (v/v).

Interference of the compounds with the colorimetric reaction was corrected for each DRC point by preparing replicate wells containing 50 µM K₂HPO₄, dissolved in the corresponding TryS master mix, and the corresponding concentrations of compounds.

IC₅₀ values were obtained from DRC (% TryS inhibition ± SD versus Log [compound] µM) fitted to a four-parameter sigmoidal equation (Boltzmann model) and expressed as IC₅₀ ± SD.

Substructure search analysis and drug-likeness analysis

The search for substructures and the drug-likeness analysis (metrics measured: FSP3, XLogP and TryS % inhibition values) for the CPA, AMTPH and AMPH scaffolds were done using the program Vortex (Dotmatics, San Diego, CA). This program was also used to search for substructures similar to compound **17** devoid of the adamantane moiety.

Cell culture and cytotoxicity assays

Bloodstream *T. brucei*

The bloodstream form of *T. brucei* (strain 427, cell line 449: encoding one copy of the tetracycline-repressor protein)²⁷ expressing the redox biosensor roGFP2 fused to human glutaredoxin-1 (hGrx1-roGFP2)²⁸ was cultivated aerobically in HMI-9 medium²⁹ supplemented with 10% (v/v) foetal bovine serum (FBS) (Gibco®, Carlsbad, CA), 1% (v/v) penicillin–streptomycin (10,000 U/mL, Gibco®), 0.2 µg/mL phleomycin (Gibco®) and 5 µg/mL hygromycin (Invitrogen™), inside a humidified incubator (Thermo Fisher Scientific) with controlled temperature (37 °C) and CO₂ (5%). Phleomycin and hygromycin were added to keep the constitutive expression of the tetracycline repressor protein and the tet-inducible hGrx1-roGFP2 gene, respectively.

The cytotoxicity of the compounds was tested according to the protocol described previously³⁰. Briefly, mid-exponential phase trypanosomes were harvested by centrifugation at 2000 *g* for 10 min at RT and resuspended at a density of 5×10^5 cells/mL in fresh

culture medium. Two hundred μL of this cell suspension were seeded per well in a 96-well culture plate (Corning 3599) containing the compound of interest at a final concentration of $25\ \mu\text{M}$ and 1% (v/v) DMSO. For compounds showing more than 90% parasite growth inhibition at $25\ \mu\text{M}$, the EC_{50} values were determined from at least 7-point concentrations. After 24 h incubation at $37\ ^\circ\text{C}$ and CO_2 (5%), $100\ \mu\text{L}$ from each well was transferred to a 2 mL tube (DELTALAB 408002) or to a 96U bottom well plate (DELTALAB 900010.1) containing $200\ \mu\text{L}$ of sterile phosphate-buffered saline (PBS)-glucose 1% (w/v) (pH 7.4), $2\ \mu\text{g}/\text{mL}$ propidium iodide (PI). The samples were immediately acquired with an AccuriTM C6 (BD) device equipped with the following laser/filter pairs: λ_{ex} 488 nm/ λ_{em} 613/30 nm and the data analysed with the Accuri C6 software (BD, Franklin Lakes, NJ).

The controls included, a positive control with Nifurtimox (Lampit[®] from Bayer) tested at its EC_{50} ($15\ \mu\text{M}$) and a proliferation control with DMSO 1% (v/v). All conditions were tested by triplicate. The relative percentage of viable parasites is expressed as: viability (%) = [(number of PI negative parasites for compound X at concentration Y)/(number of PI negative parasites in the proliferation control) \times 100%. EC_{50} values with errors expressed as one SD were obtained from DRC fitted to a dose–response (variable slope) equation using GraphPad software (GraphPad Software, La Jolla, CA).

Intracellular *L. donovani*

THP-1 (TIB-20TM) cells and parasites, were cultured in Roswell Park Memorial Institute 1640 Medium (Gibco[®]) supplemented with 10% FBS (Gibco[®]), 1% (v/v) penicillin–streptomycin ($10,000\ \text{U}/\text{mL}$, Gibco[®]) at $37\ ^\circ\text{C}$ in 5% CO_2 . For the assay, THP-1 cells were washed with media once and plated directly to 384-well μCLEAR [®] plate (Greiner Bio-One 781091) containing $50\ \text{ng}/\text{mL}$ phorbol 12-myristate 13-acetate at 1.0×10^4 cells per well and incubated for 48 h. For the infection, the metacyclic form of *L. donovani* MHOM/ET/67/HU3 was purified from stationary phase cultures ($\sim 3 \times 10^7$ parasites/mL, day 4 after inoculation) by incubating the cells with Lectin from *Arachis hypogaea* (peanut) at $50\ \mu\text{g}/\text{mL}$ for 30 min and $28\ ^\circ\text{C}$ in a shaker. Then parasites were washed twice with Dulbecco's phosphate-buffered saline (Gibco[®]) with intermediate centrifugations at $40g$ for 5 min and the parasite density was quantified prior to cell infection. Next, THP-1 cells were infected with metacyclic *L. donovani* at a multiplicity of infection 1:20. Twenty-four hours after infection, test compounds were added and the plates further incubated for 96 h. Thereafter, all wells were treated with $5\ \mu\text{M}$ of DRAQ5TM (Biostatus) and 4% (w/v) paraformaldehyde. For DRC studies, compounds were tested in duplicate at 10-point concentrations (1:2 serial dilutions of the highest concentration tested: $100\ \mu\text{M}$). Amphotericin B deoxycholate (Sigma-Aldrich, A9528) was used as reference drug tested in triplicate from 10-point concentrations. DMSO at 0.5% (v/v) was included as proliferation control. See below section **Image-based analysis** for further details on assay read-out and analysis.

Intracellular *T. cruzi*

Cells U-2 OS and LLC-MK2 were cultured in Dulbecco's modified Eagle's medium (DMEM) with high-glucose (Gibco[®]) supplemented with 10% FBS (Gibco[®]), 1% (v/v) penicillin–streptomycin ($10,000\ \text{U}/\text{mL}$, Gibco[®]) at $37\ ^\circ\text{C}$ in 5% CO_2 . LLC-MK2 was used to produce the highly infective trypomastigote forms of *T. cruzi* (strain Y) and the U-2 OS cells were used as host cells for the screening assays. Tissue culture trypomastigotes (TCTs) of *T. cruzi* were harvested from culture supernatant of LLC-MK2 infected cells (on day 7

post-infection) by centrifugation at $2000g$ for 5 min. A cell suspension containing U-2 OS cells and TCTs at a multiplicity of infection 1:12.5 was incubated with gentle swirling for 5 min. The cell mixture was then seeded ($50\ \mu\text{L}$) into a 384-well μCLEAR [®] plate (Greiner Bio-One 781091) containing test compounds. After 72 h, the cells and parasites were stained using $5\ \mu\text{M}$ of DRAQ5TM (Biostatus, Loughborough, UK) and fixed with 4% (w/v) paraformaldehyde.

For DRC studies, compounds were tested in duplicate at 10-point concentrations (1:2 serial dilutions of the highest concentration tested: $100\ \mu\text{M}$). Benznidazole (ChunyangTech, FB64954) was used as reference drug at its EC_{100} $400\ \mu\text{M}$. See below section **Image-based analysis** for further details on assay read-out and analysis.

Image-based analysis

For the *L. donovani* and *T. cruzi* bioassays, images of 4 fields/well, which correspond to a 45% coverage of the well, were acquired with the Operetta CLS confocal microscope (Perkin Elmer) at $20\times$ magnification. The images were analysed with the ColumbusTM software (Perkin Elmer) and the number of mammalian cells and intracellular parasites (recognized by the DRAQ5TM nuclei staining) were quantified to estimate EC_{50} and CC_{50} values (expressed as mean \pm one SD), respectively, from DRC plots fitted to a dose–response (variable slope) equation. GraphPad Prism6 (GraphPad Software, San Diego, CA) was used for the analysis of quantitative data.

Redox assays for bloodstream *T. b. brucei*

Bloodstream *T. brucei brucei* (strain 427, cell line 449) expressing the redox biosensor hGrx1-roGFP2 was cultivated as indicated above and 24 h prior to the redox assays, the expression of the reporter gene was induced by adding $1\ \mu\text{g}/\text{mL}$ oxytetracycline to the culture medium. Induced parasites in exponential growth phase were harvested by centrifugation and resuspended in fresh medium at a density of 2×10^6 cells/mL. Two hundred μL of this cell suspension were seeded per well in a 96-well plate and incubated (5% CO_2 and $37\ ^\circ\text{C}$ for 4 h) with the compound of interest added a $1\times$ and $2\times$ its EC_{50} . Control conditions included parasites treated with DMSO 1% (v/v) for 4 h, and DTT (1 mM), menadione ($250\ \mu\text{M}$) or diamide ($250\ \mu\text{M}$) for 20 min. All conditions/compounds were tested in triplicates. Next, $100\ \mu\text{L}$ from each well were transferred to a tube containing $200\ \mu\text{L}$ of sterile PBS with glucose 1% (w/v) and $2\ \mu\text{g}/\text{mL}$ PI. All samples were analysed with an AccuriTM C6 flow cytometer and the following laser/filter pairs: λ_{ex} 488 nm/ λ_{em} 613/30 nm for PI and λ_{ex} 488 nm/ λ_{em} 530/40 nm for GFP. A maximum of 10,000 events was acquired per sample. The mean fluorescence intensity (MFI; PI and GFP) of the samples was normalised to the corresponding fluorescence reference values of parasites incubated in the presence of DMSO 1% (v/v) and DTT. The level of roGFP2 mean fluorescence intensity was analysed only for samples presenting $> 40\%$ viable cells (PI negative). The relative level of biosensor reduction was calculated as follows: % biosensor reduction = [(MFI hGrx1-roGFP2 for compound X at concentration Y)/(MFI hGrx1-roGFP2 for DMSO 1% (v/v) with DTT) – (MFI hGrx1-roGFP2 for menadione)] \times 100%.

For compounds inducing changes in roGFP2 fluorescence, DTT (1 mM) or menadione ($250\ \mu\text{M}$) was added to the sample and, after 20 min incubation at RT, re-analysed by flow cytometry as indicated above.

The data were processed and analysed with the Accuri C6 software. Plots were prepared with the GraphPad software and errors expressed as one SD.

Inhibition mode of candidate hits against TbTryS

Time-dependent assays

Under identical assay conditions described in section **High-throughput TryS assay**, 5 μM Ebselen (IC_{50} for TbTryS) (stocks prepared at 80 μM in water with DMSO 20% v/v) was pre-incubated for 1 h at 28 °C with: TbTryS (6.1×10^{-6} $\mu\text{mol}/\text{min mL}$; Sample A) or MM (Sample B). Next, MM and TbTryS were added to sample A and B, respectively, and a reaction (Sample C) containing Ebselen (5 μM), TbTryS (6.1×10^{-6} $\mu\text{mol}/\text{min mL}$) and MM was prepared. All samples were incubated for 1 h at 28 °C and then BIOMOL GREENTM reagent was added to detect Pi formation. $A_{620\text{nm}}$ was measured with a MultiScan FC plate reader (Thermo Fisher Scientific). Control samples (TbTryS+MM) lacking Ebselen were run in parallel. All conditions were tested in 6 replicates and data analysed as described in the aforementioned section.

Dilution and reduction-based assays

TbTryS (1.44 μM , 2.4×10^{-5} $\mu\text{mol}/\text{min.mL}$) and 10 μM Ebselen (stock prepared at 100 μM in water with DMSO 20% v/v) were mixed and incubated during 1 h at 20–23 °C. Thereafter, the excess compound was removed with a Zeba Spin Desalting Column 7 kDa Molecular Weight Cut-Off (Thermo Fisher Scientific) previously equilibrated with reaction buffer. Next, samples (10 μL) were incubated for 30 min in the absence or presence of DTT 5 mM for 30 min at 28 °C. TryS activity was measured in a 384-plate upon diluting the samples in reaction buffer (1:2 dilution) and incubating for 1 h at 28 °C with MM added or not of DTT 5 mM (stock prepared at 80 mM in reaction buffer), respectively. Controls with and without enzyme along with DMSO at 2% (v/v) were included. The reaction was stopped with the addition of the BIOMOL GREENTM reagent. The absorbance was measured at 620 nm with a MultiScan FC plate reader (Thermo Fisher Scientific). Six replicates were tested per sample and the % TryS inhibition calculated as indicated in the section **High-throughput TryS assay**.

Mass spectrometry assays

In order to identify the residue of TbTryS that is target of covalent modification by Ebselen, 100 μL samples containing 1.44 μM recombinant enzyme (2.4×10^{-5} $\mu\text{mol}/\text{min mL}$) in TryS reaction buffer were prepared and incubated for 1 h with: (A) Ebselen 20 or 50 μM (stocks prepared at 200 or 500 μM in water with DMSO 20% v/v), (B) 15 mM iodoacetamide (IAM, 500 mM stock solution prepared in distilled water) or (C) DMSO 2% v/v. Next, samples (A) and (B) were desalted using a Zeba Spin Desalting Column 7 kDa Molecular Weight Cut-Off (Thermo Fisher Scientific) pre-equilibrated in distilled water and then treated for 1 h with 15 mM IAM. All steps were performed at 20–23 °C.

TryS activity (8 replicates) was determined in all samples after the first hour of incubation as described in the previous section. Equal amounts of protein (~0.011 mg) were adjusted to pH 8.0 with 50 mM ammonium bicarbonate and digested overnight at 37 °C using sequencing grade trypsin (Promega, Madison, WI) at a final protease:protein ratio of 1:20 (w/w). The digestions were then acidified with 10% trifluoroacetic acid up to a final concentration of 1%. Peptide samples were concentrated under vacuum in

a CentriVap concentrator (LabconoTM) and desalted using ZipTip[®] C18 tips (Merck Millipore, Kenilworth, NJ). Eluted peptides were finally resuspended with 0.1% formic acid in liquid chromatography/mass quality water (LiChrosolv[®], Merck KGaA).

Liquid chromatography-MS/MS analysis was performed with an UltiMate 3000 liquid chromatography system (Thermo Fisher Scientific) coupled to a Q Exactive Plus mass spectrometer equipped with an Easy-SprayTM source (Thermo Fisher Scientific). Samples were loaded into a precolumn (AcclaimTM PepMapTM 100, C18, 75 $\mu\text{m} \times 2\text{cm}$, 3 μm particle size, Thermo Fisher Scientific) and separated with an Easy-SprayTM analytical column (PepMapTM RSLC, C18, 75 $\mu\text{m} \times 50\text{cm}$, 2 μm particle size, Thermo Fisher Scientific) at 40 °C using a two-solvent system: (A) 0.1% formic acid in water and (B) 0.1% formic acid in acetonitrile. Column was equilibrated at 1% B followed by a gradient elution performed as follows: 1–50% B for 115 min, 50–99% B for 10 min, 99% B for 5 min and 1% A for 10 min, with a constant flow rate of 200 nL/min. The mass spectrometer was operated in a positive mode. Ion spray voltage was set at 2.5 kV; capillary temperature at 250 °C and S-lens radio frequency level 50. A top-12 data-dependent method was used for mass data acquisition. Full mass scans were acquired in a range of 200–2000 m/z with a resolution of 70,000 at 200 m/z , automatic gain control target value of 1×10^6 and a maximum ion injection time of 100 ms. Precursor fragmentation occurred in a high-energy collision dissociation cell with a resolution of 17,500 at 200 m/z , automatic gain control target value of 1×10^5 and a maximum ion injection time of 50 ms. Normalised collision energy was used in a stepped mode (25, 30 and 35). Precursor ions with single, unassigned or eight and higher charge states were excluded. A dynamic exclusion time was set to 30 s.

Computational analysis

PatternLab for Proteomics 4.0 (PatternLab) software was used to process raw data files³¹. The sequence of recombinant TbTryS was added to the *Escherichia coli* proteome downloaded from Uniprot on July 2020 (<http://www.uniprot.org/>) and a target-reverse database was generated using PatternLab. The most common contaminants in Proteomics experiments were also included in the database. Search parameters were set as follows: methionine oxidation, cysteine di and tri oxidation, cysteine carbamidomethylation, and Ebselen covalent modification (+274.985 Da) in cysteine/lysine were defined as variable modifications. A maximum of 2 missed cleavages and 3 variable modifications per peptide were allowed. Search results were filtered by PatternLab Search Engine Processor algorithm with a maximum false discovery rate value $\leq 1\%$ at protein level. The inspection of the MS/MS spectra of Ebselen-modified peptides identified by Patternlab allowed us to recognise a very characteristic fragmentation pattern dominated by the release of Ebselen modification and the presence of low intensity sequence ions. This fragmentation behaviour might result in low confidence assignment of spectrum to peptide sequences. To cover possible modification sites not identified by the search engine, we rely on the presence of the Ebselen modification reporter ions (an intense signal of $m/z = 275.9938$ corresponding to protonated Ebselen plus 2 fragmentation products of $m/z = 196.0751$ and 183.9417) (<https://mona.fiehnlab.ucdavis.edu/spectra/display/FiehnHILIC001906>). Raw data were mass filtered using Thermo Scientific XcaliburTM 4.0 software to identify MS/MS spectra containing these ions, and the putative modification by Ebselen was further manually validated. Mass spectrum were plotted using OriginPro 8 software. The mass spectrometry proteomics data have been deposited to the ProteomeXchange Consortium

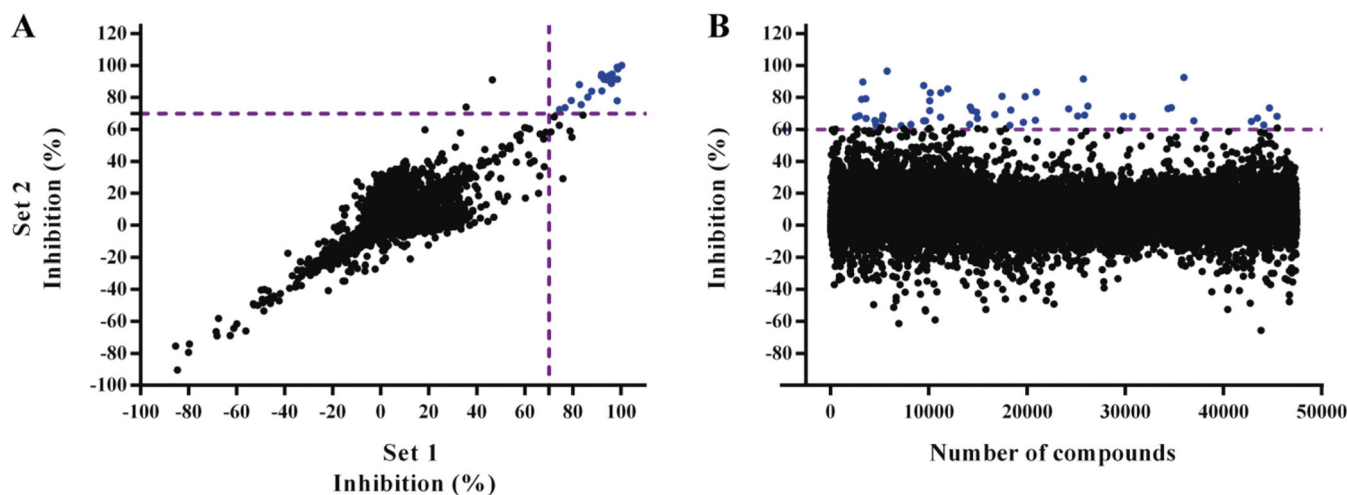


Figure 2. HTS screening against *Trypanosoma brucei* Trypanothione synthetase (*TbTryS*). (A) Pilot screening. An *in-house library* of 4210 compounds was tested at 25 μM , and in duplicate in two independent experiments (indicated as Set 1 and Set 2), for their inhibitory activity against *TbTryS*. Linear regression fitting for *TryS* inhibition (%) from both sets yielded a R^2 value of 0.96. Twenty compounds displayed $\geq 70\%$ enzyme inhibition (blue dots), which corresponds to a hit ratio of 0.47%. (B) Large screening. A commercial library of 47,414 small compounds (*ENAMINE*) was tested at 25 μM for their inhibitory activity against *TbTryS*. Sixty-two compounds displayed $\geq 60\%$ enzyme inhibition (blue dots), which corresponds to a hit ratio of 0.13%.

via the PRIDE³² partner repository with the dataset identifier PXD027729.

Kinetic mechanism of inhibition

Assays were conducted at 28 $^{\circ}\text{C}$, using 384-well plates and a total reaction volume of 16 μL , 1 μL of compound **17** or DMSO 20% and 5 μL of MM. Compound and *TbTryS* were incubated for 60 min, then the reaction was started by adding 5 μL MM and stopped after 60 min with 60 μL BIOMOL GREENTM reagent. The colorimetric reaction was allowed to develop for 20 min and then absorbance at 620 nm was measured with a MultiScan FC plate reader (Thermo Fisher Scientific).

Before running the kinetic studies, the enzyme concentration was adjusted in order to obtain a linear relationship at optimal substrates concentration for *TbTryS* (4.5 mM SP or 100 μM Gsp, 150 μM GSH and 200 μM ATP; max. $A_{620\text{nm}} \sim 0.5$; $\sim 75 \mu\text{M}$ Pi), which corresponded to an enzyme activity of $3.3 \times 10^{-5} \mu\text{mol}/\text{min.mL}$ with SP or $2.6 \times 10^{-5} \mu\text{mol}/\text{min.mL}$ with Gsp.

Compound **17** was tested at the following concentrations: 0, 0.625-, 1.25-, 2.5-, 5-, 10- and/or 20-folds its IC_{50} . Due to substrate inhibition by GSH²⁵ the assays were performed at 150 μM for GSH ($\sim K_M$ value), whereas SP, Gsp and ATP were added at 4.5 mM (~ 19 -fold the K_M value), 100 μM (~ 42 -fold the K_M value)³³ and 200 μM (~ 10 -fold the K_M value), respectively. When GSH was the variable substrate, the concentrations ranged from 600 to 75 μM . When ATP was the variable substrate, the concentrations tested ranged from 200 to 75 μM . For SP, the concentrations were varied from 4.5 to 0.167 mM. Gsp was tested at a fixed concentration of 100 μM .

All tests were performed in seven replicates for each concentration of compound evaluated. A single blank per condition was prepared by adding 10 μL of screening reaction buffer instead of enzyme.

The assays were run manually and yielded an intra-assay coefficient variation $\leq 10\%$. Lineweaver-Burk plots ($1/[\text{Abs}]$ versus $1/[\text{substrate}]$) were prepared and analysed using the OriginPro 8 software. An R -square (R^2) ≥ 0.96 was used as criteria to eliminate outliers for fitting plots. For ATP, GSH and SP the fitting was performed using a linear, an exponential ($y = y_0 + A \times e^{R \times X}$) and a sigmoideal [$y = (V_{\text{max}} \times X^n)/(K^n + X^n)$] equation, respectively.

Results

Identification of *TryS* inhibitors

A pilot screening with 4210 compounds from the LOPAC[®] (SIGMA), Selleck Chemicals, NIH Clinical and TOCRIS libraries (from now on named: *in-house library*), all of them with well-known biochemical and physiological activities, was performed in duplicate to assess the robustness and reproducibility of the 384-well plate screening assay. The Z' factor³⁴ for the set 1 and set 2 was 0.78 and 0.79, respectively, and the R^2 value obtained for the plot from both assays sets was 0.96. These results confirmed the suitability of the HTS assay for running a screening with a larger number of compounds. For this preliminary screening, a *hit* was defined as a compound exerting $\geq 70\%$ *TbTryS* inhibition at 25 μM . Twenty compounds fulfilled this criterion, which yielded a hit ratio of 0.47% (Figure 2(A)).

Based on the robustness of the miniaturised screening assay, next, a large HTS was performed with a commercial library (*ENAMINE*) consisting of 47,414 drug-like compounds of wide chemical diversity. The compounds were tested once at a single point concentration of 25 μM . For practical reasons, the screening was divided into three runs that overall rendered an average Z' factor of 0.83 and a signal-to-background value of 8.07. For this assay, the cut-off for a hit was set at $\geq 60\%$ *TbTryS* inhibition, which yielded 62 compounds and a hit ratio of 0.13% (Figure 2(B)).

Thus, a total of 82 hit candidates from the *in-house* and the *ENAMINE* libraries were re-purchased and, with the aim to identify multi-species *TryS* inhibitors, tested at 25 μM against *TryS* from *T. brucei*, *T. cruzi* and *L. infantum* (Tri-Tryp *TryS*; Table S1). Twenty-five out of the 82 potential hits were confirmed as true inhibitors of *TbTryS* with IC_{50} values ranging from 1.2 to 36.2 μM (Table 1).

Interestingly, the hit confirmation ratio for *TbTryS* was higher for compounds belonging to the *in-house library* (10 out of 20 hit candidates: 50% hit ratio) than for those from the *ENAMINE* library (15 out of 62 hit candidates: 24% hit ratio). This difference can be ascribed to the fact that compounds from the pilot-screening were tested in duplicates whereas those from the *ENAMINE* library were assayed in uniplicates. Interestingly, extending the screening of the 82 hits *TbTryS* hit candidates to the related enzymes from *T. cruzi* and *L. infantum* led to the identification of several

Table 1. Hit compounds targeting trypanothione synthetase (TryS) inhibition.

| # ^c | Compound | Core scaffold ^d | % TryS inhibition at 25 μM^a or IC_{50} (μM) ^b | | |
|----------------|-----------------------------|----------------------------|--|-------------------|--------------------|
| | | | <i>T. brucei</i> | <i>T. cruzi</i> | <i>L. infantum</i> |
| 1 | Aurintricarboxylic acid | Singleton | 8.2 ± 0.6 | 5.5 ± 2.8 | 4.6 ± 0.7 |
| 2 | 4-Chloromercuribenzoic acid | Singleton | 2.20 ± 0.05 | 32.0 ± 9.7 | NA |
| 3 | 6-Hydroxy-DL-DOPA | Singleton | 13.0 ± 3.5 | 16.8 ± 2.8 | 4.0 ± 1.4 |
| 4 | NH125 | Singleton | 12.0 ± 2.5 | 15.5 ± 2.9 | 25.7 ± 2.6 |
| 5 | Ebselen | Singleton | 5.3 ± 0.2 | 13.8 ± 1.5 | 2.6 ± 0.2 |
| 6 | Sanguinarine chloride | Singleton | 3.3 ± 0.4 | 40.0 ± 1.2 | 11.6 ± 0.4 |
| 7 | Calmidazolium chloride | Singleton | 9.5 ± 2.5 | 2.7 ± 0.5 | 1.6 ± 0.8 |
| 8 | SCH 202676 hydrobromide | Singleton | 3.7 ± 0.5 | 43.4 ± 5.7 | 3.0 ± 0.8 |
| 9 | PD 404,182 | Singleton | 15.3 ± 1.1 | 10.9 ± 5.6 | 8.9 ± 5.9 |
| 10 | Demethylasterriquinone B1 | Singleton | 31.0 ± 7.0 | 27.7 ± 7.6 | 69.3 ± 3.5 |
| 11 | CGP 71683 hydrochloride | Singleton | 14.4 ± 8.2 | 34.7 ± 7.6 | 13.9 ± 1.8 |
| 12 | PQ 401 | Singleton | 1.5 ± 0.4 | 6.2 ± 5.6 | NA |
| 13 | WIN 64338 hydrochloride | Singleton | 9.2 ± 7.4 | 25.9 ± 6.5 | 70.9 ± 6.8 |
| 14 | Z109494586 | Singleton | 8.0 ± 1.8 | 7.1 ± 4.0 | 16.8 ± 17.9 |
| 15 | Z1188133056 | Singleton | ~25 ^c | NA | NA |
| 16 | Z13601063 | Singleton | 28.0 ± 4.5 | NA | NA |
| 17 | Z147103388 | Singleton | 1.2 ± 0.2 | NA | NA |
| 18 | Z1547375509 | Singleton | 15.2 ± 3.7 | NA | 28.5 ± 11.1 |
| 19 | Z21459859 | Singleton | 36.2 ± 2.6 | 13.3 ± 3.3 | NA |
| 20 | Z225233562 | AMTPH | 20.3 ± 4.6 | NA | NA |
| 21 | Z227072034 | AMTPH | 8.4 ± 0.9 | NA | NA |
| 22 | Z227978766 | Singleton | NA | 12.9 ± 6.1 | 8 |
| 23 | Z244772346 | AMPh | 28.2 ± 1.3 | NA | NA |
| 24 | Z318180488 | AMPh | 13.1 ± 0.7 | NA | NA |
| 25 | Z339866610 | CPA | 26.4 ± 0.9 | NA | NA |
| 26 | Z363062290 | CPA | 18.4 ± 2.5 | 8.8 ± 7.3 | NA |
| 27 | Z51971326 | AMTPH | 19.9 ± 2.7 | NA | NA |
| 28 | Z572699208 | CPA | ~25 ^c | NA | NA |
| 29 | Z95976280 | CPA | 12.0 ± 2.6 | NA | NA |

^a% TryS inhibition is expressed as the mean ± standard deviation, where NA, denotes “not active” (i.e. TryS inhibition $\leq 0.0 \pm 5.0\%$ at 25 μM).

^bValues in italic and bold refers to IC_{50} . For compounds showing TryS inhibition of 45–55% at 25 μM , the IC_{50} was approached to ~25 μM .

^cCompounds 1–13 (grey background) and 14–29 correspond to hits from the *in-house* and *ENAMINE* library, respectively.

^dCPA: Carboxy piperidine amide; AMTPH: amide methylene thiazole phenyl; AMPh: amide methylene phenyl. Structural information of molecules belonging to the *ENAMINE* library can be retrieved from the company website (<https://www.enaminestore.com/search>) using the corresponding compound code.

compounds with multi-TryS inhibitory activity: 13 belonging to the *in-house library* and 16 from the *ENAMINE* library (Table 1). Strikingly, the selected hit candidates from the *ENAMINE* library showed a high selectivity for *TbTryS* (Table 1). The exception were the singletons **22** (IC_{50} 8 μM , Table 1), **46** and **82** (74% and 43% TryS inhibition; Table S1) that inhibited *LtTryS* and proved inactive or poorly active against *TbTryS* or *TcTryS*. In contrast, the *in-house library* yielded a high number of compounds with wide-spectrum inhibitory activity against Tri-Tryp TryS with IC_{50} values ranging from 1.6 to 40 μM (i.e. **3**, **4**, **5**, **6** and **7**). A few compounds displayed species-specific activity against two (**1** and **8** inhibited *LtTryS* and *TbTryS*) or a single TryS (i.e. **12** versus *TbTryS* and **13** versus *LtTryS*). Interestingly, three singletons (**10**, **11** and **13**) that were poorly active against *TbTryS* showed higher inhibitory activity towards *LtTryS*. Overall, *TcTryS* resulted the most refractory enzyme to inhibition.

Strikingly, the remarkable differences in hits' ratio and species-specificity for TryS correlated inversely with the library size and its chemical diversity. The *in-house* library consisted only of singletons (4210) with proven biochemical/biological activity and led to the identification of wide-spectrum TryS inhibitors. In contrast, the larger and more diverse *ENAMINE* library, consisting of 3753 compounds' clusters and 4332 singletons (all together totalising 47,414 compounds), led to the identification of a few and TryS species-specific inhibitor' scaffolds.

The *TbTryS* hits from the *ENAMINE* library can be clustered into three major scaffolds: (A) carbonyl piperidine amide (CPA) (4 active compounds, with 7 out of 62 exerting an inhibition $\geq 60\%$), (B) amide methylene thiazole phenyl (AMTPH) (3 active compounds, with 4 out of 62 compounds exerting an inhibition

$\geq 60\%$) and (C) amide methylene phenyl (AMPh) (2 active compounds, with 10 out of 62 exerting inhibition $\geq 60\%$) (Tables 1 and S1 and Figure 3). A substructure mining of the *ENAMINE* library delivered the following number of analogues: 255 for CPA, 47 for AMTPH and 1547 for AMPh, one being common to the last two scaffolds. Based on this information, the AMPh can be dismissed as a real active scaffold given that only 2 out of 1547 analogues (0.001%) proved active against TryS. However, the AMTPH (hit ratio = 6.4%) and the CPA (hit ratio = 2.7%) series may be considered as real active scaffolds.

The drug-likeness of the scaffolds was analysed considering the following parameters: the fraction of sp³ hybridized or saturated carbons (FSP3) and the lipophilicity (XLogP). The CPA compounds showed better drug-like properties than the other scaffolds since the FSP3 score was >0.3 (pointing to a higher molecular flexibility, as commented above) and the XLogP <5 (Figure S2). Regarding the hit singletons from the *ENAMINE* library, the most potent was **17** with an IC_{50} = 1.2 μM (Tables 1 and Figure 3). A search for related compounds revealed 24 analogues lacking the adamantane moiety (data not showed). Interestingly, none of them was active against *TbTryS* suggesting that the lipophilic adamantane moiety is relevant for anchoring the inhibitor to the enzyme active site.

Phenotypic-based screening

The most active inhibitors of Tri-Tryp TryS were tested for their biological activity against the clinically relevant forms of the corresponding trypanosomatid species: *T. brucei*, *L. donovani* and *T.*

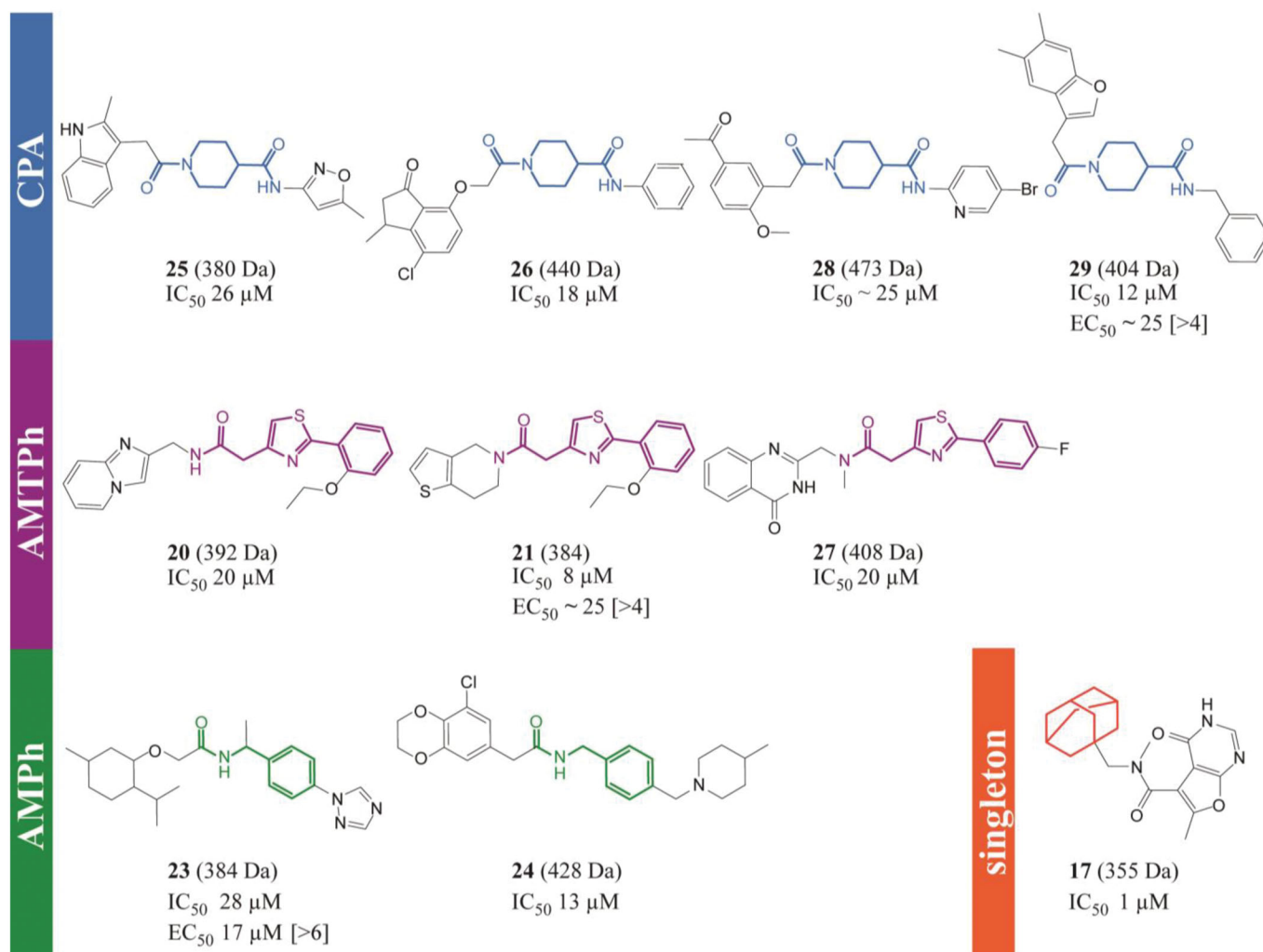


Figure 3. *T. brucei* TryS hit compounds from the ENAMINE library. CPA: carboxy piperidine amide derivatives, AMTPh: amide methylene thiazole phenyl derivatives, AMPh: amide methylene phenyl derivatives and singleton: 17, the most potent singleton with its adamantane moiety highlighted in orange. The scaffolds or moiety of interest are highlighted in different bold colours. The EC₅₀ (bloodstream *T. brucei*) and selectivity index (value in brackets, reference cell line: human macrophages, THP-1) are shown only for compounds with anti-proliferative action against *T. brucei* at concentrations ≤ 25 μM. All the errors are expressed as one SD and the compounds' molecular mass in Daltons.

cruzi (Table 2 and Figure 3 for hits from ENAMINE library and Figure 4 for hits from the in-house library).

Twenty-four compounds with IC₅₀ ≤ 36 μM against *TbTryS* (Table 1) and CC₅₀ against THP-1 ≥ 10 μM were evaluated against the bloodstream form of *T. brucei* (Table 2). Six (2, 4, 5, 7, 8 and 12) out of nine compounds from the in-house library showed good potency (EC₅₀ 0.34–8.9 μM) and remarkable cytotoxic selectivity against the pathogen (SI 11–182). Among them, 4 (EC₅₀ 0.34, SI 29) and 7 (EC₅₀ 0.55, SI 182) resulted the top biological hits (Table 2). In contrast, five (two singletons: 14 and 19, and one from each main inhibitor scaffold AMPH: 23, AMTPh: 21 and CPA: 29) out of fifteen compounds from the ENAMINE library showed moderate activity (EC₅₀ 5–25 μM) and poor selectivity (SI > 4 to 11) against *T. brucei* (Table 1 and Figure 3).

Compounds with an IC₅₀ ≤ 40 μM against *TcTryS* (3, 4, 5, 6 and 7) were evaluated against the intracellular form of *T. cruzi* infecting human osteosarcoma cells (cell line U-2 OS). Except for 3 (EC₅₀ 34 μM), the other compounds showed low (sub)μM potency (EC₅₀ 0.4–2.8 μM). The four most active compounds against *T. cruzi* displayed a higher toxicity towards the osteosarcoma cells (selectivity index = SI 1.1–2.6) than against human macrophages (SI 9.5 to >56), which are also physiological hosts for this pathogen.

Finally, 11 compounds showing IC₅₀ < 26 μM against *LtTryS* (1, 3, 4, 5, 6, 7, 8, 10, 11, 13 and 22) (Table 1) were evaluated against the intracellular form of *L. donovani* hosted by human macrophages (cell line THP-1). Three of these compounds (4, 6 and 10) displayed activity against the pathogen at low μM concentrations (EC₅₀ 1.7–4.5 μM) and with a remarkable poor selectivity (SI 1.6–3). Three additional compounds (8, 11 and 13) were one order of magnitude less potent (EC₅₀ 26–56 μM) and with almost negligible selectivity (SI 1.1–1.9) (Table 2).

Correlation between on-target (in vitro TryS inhibition) and anti-trypansomatid activity of selected TryS hits

The compounds tested in our study have drug-like properties (low molecular weight, cell permeability and/or, some of them, proven bioactivity), which allow to comparatively analyse their IC₅₀ and EC₅₀ to establish a potential correlation in bioactivity (Figure 5). Twelve of the *TbTryS* hits presented higher inhibitory activity towards the molecular target than against the parasite (Figure 5(A), black symbols), seven showed a good correlation between target inhibition and anti-*T. brucei* activity (2, 8, 15, 16, 20, 25 and 28, red symbols), whereas five compounds proved more

Table 2. Biological activity of TryS inhibitors against the infective stage of different trypanosomatids (bloodstream *T. brucei* and intracellular amastigotes of *T. cruzi* and *L. donovani*) and mammalian (host) cells.

| Compound ^c | Cytotoxicity (EC ₅₀ μM) ^a and selectivity index [SI] ^b | | |
|-----------------------|---|---|---|
| | <i>T. brucei</i> ^d [SI vs. THP-1] | <i>T. cruzi</i> ^d [SI vs. U-2 OS/THP-1] | <i>L. donovani</i> ^d [SI vs. THP-1] |
| 1 | >25 | ND | >100 |
| 2 | 2.1 ± 0.2 [48] | ND | ND |
| 3 | >25 | ~34 [2.7 / >2.7] | >100 |
| 4 | 0.34 ± 0.01 [29] | 0.56 ± 0.01 [2.6 / ~18] | 3.2 ± 0.6 [~3] |
| 5 | 8.9 ± 0.7 [11] | 2.8 ± 0.1 [2.4 / >36] | >100 |
| 6 | ND | 0.37 ± 0.11 [1.3 / 9.5] | 1.7 ± 0.2 [2] |
| 7 | 0.55 ± 0.03 [182] | 1.6 ± 0.1 [1.1 / >55.6] | >100 |
| 8 | 4.6 ± 0.5 [20] | ND | ~ 56 [~1.4] |
| 9 | >25 | ND | ND |
| 10 | ND | ND | 4.5 ± 0.7 [1.6] |
| 11 | ND | ND | 26.0 ± 8.1 [1.1] |
| 12 | 5.9 ± 0.5 [14] | ND | ND |
| 13 | ND | ND | 31 ± 5 [1.9] |
| 14 | 5.2 ± 3.2 [11] | ND | ND |
| 15 | >25 | ND | ND |
| 16 | >25 | ND | ND |
| 17 | >25 | ND | ND |
| 18 | >25 | ND | ND |
| 19 | ~20 [>4] | ND | ND |
| 20 | >25 | ND | ND |
| 21 | ~25 [>4] | ND | ND |
| 22 | ND | ND | >100 |
| 23 | 17.1 ± 4.4 [>6] | ND | ND |
| 24 | >25 | ND | ND |
| 25 | >25 | ND | ND |
| 26 | >25 | ND | ND |
| 27 | >25 | ND | ND |
| 28 | >25 | ND | ND |
| 29 | ~25 [>4] | ND | ND |
| Nifurtimox | 15.0 ± 2.5 | ND | ND |
| Benznidazole | ND | 2.5 ± 0.2 [>40] | ND |
| Amphotericin B | ND | ND | 0.18 ± 0.02 [>22] |

^aThe effect of the compounds in trypanosomatids viability is expressed as EC₅₀ (half-maximum effective concentration). The values correspond to the mean ± SD (*n* = 3). For some compounds the EC₅₀ reported corresponds to the closest concentration reducing cell viability to 45–55% and is indicated with the symbol “~”.

^bThe selectivity index is calculated as the quotient CC₅₀ (half-maximum mammalian cytotoxic concentration)/EC₅₀ for the indicated host cell/pathogen pair.

^cCompounds 1–13 (grey background) and 14–29 correspond to hits from the *in-house* and *ENAMINE* library, respectively.

^dND: not determined.

active in killing the pathogen (**4**, **7**, **14**, **19** and **23**, blue symbols). In contrast, only two TryS hits, one *per* parasite species, showed a good correlation between IC₅₀ and EC₅₀ for the intracellular pathogens *T. cruzi* (**7**, Figure 5(B)) and *L. infantum* (**13**, Figure 5(C)). Three of the *Tc*TryS hits tested proved more active in killing the parasite than in inhibiting the enzyme (**4**, **5** and **6**), and only one (**3**) showed the opposite behaviour. Most of the *Li*TryS hits proved to be far more active against the enzyme than towards the pathogen (**1**, **3**, **5**, **7**, **8**, **11** and **22**) and three showed a comparatively higher potency against the parasite (**4**, **6** and **10**). Interestingly, the linear correlation between IC₅₀ versus EC₅₀ exhibited by some compounds was species specific. This does not necessarily suggest a lack of conserved on-target effect of the hits but may, at least in part, be attributed to differences in the capacity of the compounds to achieve effective intracellular concentrations in pathogens that dwell in different environments (*T. brucei*: extracellular, *T. cruzi*: host cell cytosol, and *L. infantum*: host cell endolysosome).

Notably, against trypanosomes, seven and five of the *Tb*TryS and *Tc*TryS hits, respectively, qualified also as biological hits according to official criteria (EC₅₀ ≤ 10 μM and SI > 10)³⁵.

Assays with redox-reporter cell line of bloodstream *T. brucei*

Inhibition of trypanothione synthesis either by genetic^{6,7} or chemical^{9,12,13} approaches leads to an intracellular oxidative milieu due to exhaustion of the antioxidant system to cope with the elimination of endogenous peroxides caused by trypanothione depletion.

In order to provide preliminary evidence on the on-target effect of the TryS's hit displaying anti-proliferative activity against *T. brucei* (EC₅₀ ≤ 25 μM and IC₅₀ ≤ 25 μM), their capacity to alter the intracellular redox state of the parasites was addressed using a redox-reporter cell line of bloodstream *T. b. brucei*. The transgenic cell line expresses a GFP-based redox biosensor (roGFP2)²⁸ that allows monitoring non-invasively, and in a dynamic fashion, perturbations in the pool of reduced and oxidised low molecular weight thiols (i.e. GSH/GSSG and T(SH)₂/TS₂)³⁶. For instance, a high fluorescence intensity of roGFP2 excited at 488 nm indicates a reducing intracellular milieu (i.e. high GSH/GSSG or T(SH)₂/TS₂ ratio) whereas a decrease in roGFP2 fluorescence intensity (Ex 488 nm) points to an oxidising intracellular milieu (i.e. low GSH/GSSG or T(SH)₂/TS₂ ratio). This redox reporter cell line was successfully used to study the anti-trypanosomal mode of action of different families of compounds^{37–42}.

Bloodstream *T. b. brucei* expressing the redox biosensor was treated with the most potent compounds targeting TryS and *T. brucei* (EC₅₀ ≤ 25 μM and IC₅₀ ≤ 25 μM: **2**, **4**, **5**, **7**, **8**, **12**, **14**, **21**, **23** and **29**) added at concentrations corresponding to 1× or 2× their EC₅₀ (Table 2). After 4 h exposure, the fluorescence intensity of roGFP2 was analysed by flow cytometry for parasites exhibiting membrane integrity (PI negative cells). The redox analysis was not performed for **7**, **21** and **23** at 2× their EC₅₀ because of the massive cell death they caused. As shown in Figure 6(A), and compared to the vehicle treated control (1% v/v DMSO), only compound **5** (Ebselen) added at 18 μM (2-fold its EC₅₀) induced a 48% oxidation of the biosensor upon 4 h treatment that was reverted by exposing the parasites to the membrane permeant reducing agent DTT (1 mM for 20 min, Figure 6(B)).

Strikingly, at 2-fold its EC₅₀, compound **4** increased significantly biosensor fluorescence at a value 45% above that obtained under fully reducing conditions (1 mM DTT). In order to verify the redox basis of this phenomena, a fraction of this sample was treated with the oxidising agent menadione under conditions that in vehicle alone treated parasites cause full biosensor oxidation (250 μM menadione for 20 min; Figure 6(A)). This treatment caused an oxidation of the biosensor (i.e. from 145% to 62% biosensor reduction, drop of 83%) of similar magnitude to that induced in vehicle-alone treated cells (i.e. from 82% to 0% biosensor reduction, drop of 82%). This clearly indicates that compound NH125 is not reducing the biosensor at intracellular level but increasing the background level of (auto)fluorescence. Altogether, these data suggest that Ebselen is the only TryS' hit whose mechanism of parasite killing involves the generation of a decrease in the ratio of reduced vs. oxidised low molecular weight thiols upon a short time exposure.

Mode of inhibition of *Tb*TryS by Ebselen

Ebselen was chosen for further mechanistic studies because it was one of the few compounds displaying multi-species TryS inhibitory activity (Table 1) and anti-proliferative action against the infective stages of *Trypanosoma* (Table 2) by rapidly inducing the generation of an intracellular oxidative milieu (Figure 6).

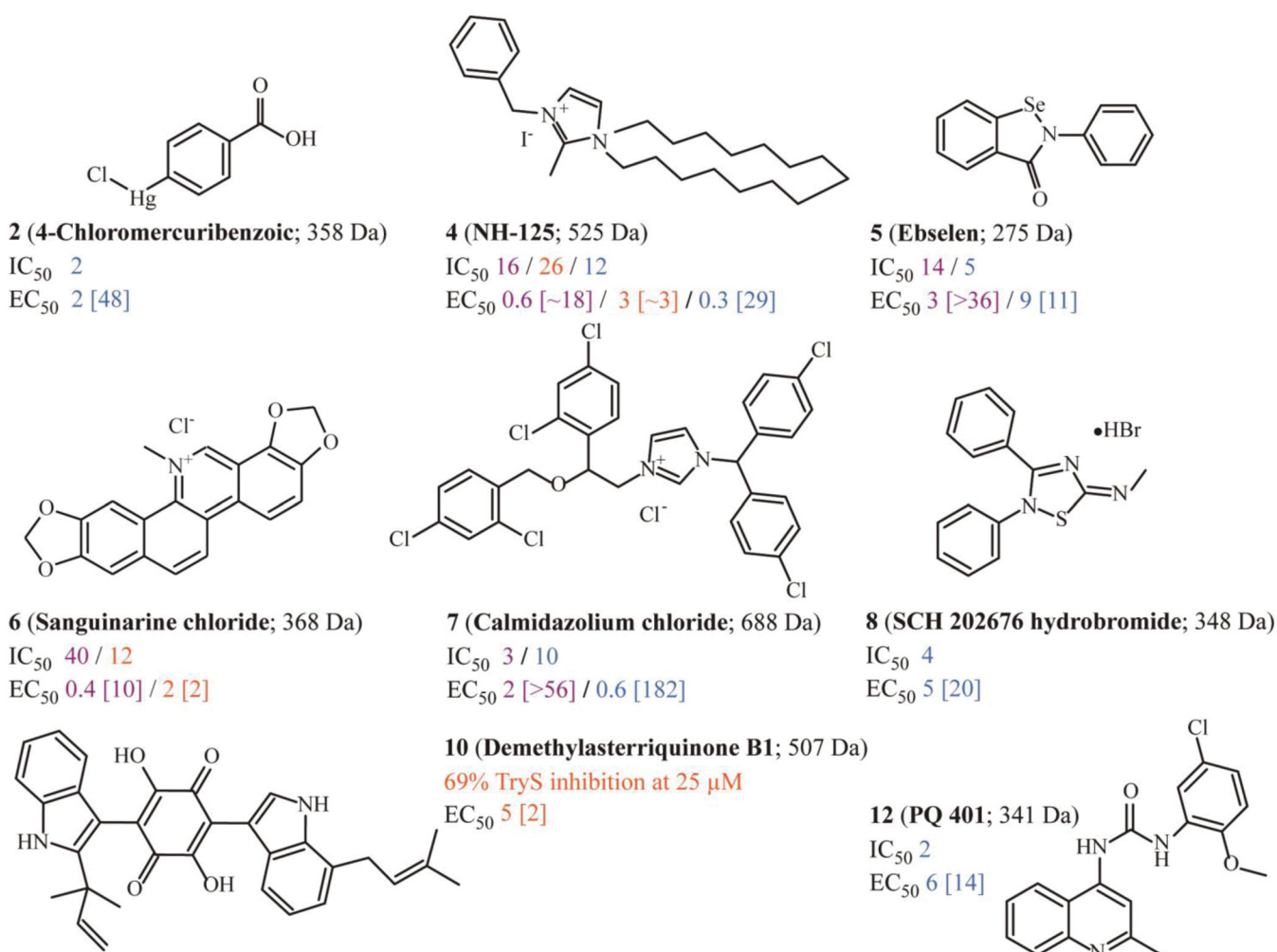


Figure 4. Most prominent TryS hits from the *in-house library* tested against the clinically relevant forms of major trypanosomatid species. Compound's structure, molecular weight (in Daltons) and activity (IC_{50} and EC_{50} are in μ M units, and the selectivity index is referred to human macrophages and shown within brackets). The biodata is highlighted in blue for *T. brucei*, violet for *T. cruzi* and orange for *Li-TryS* or *L. donovani*.

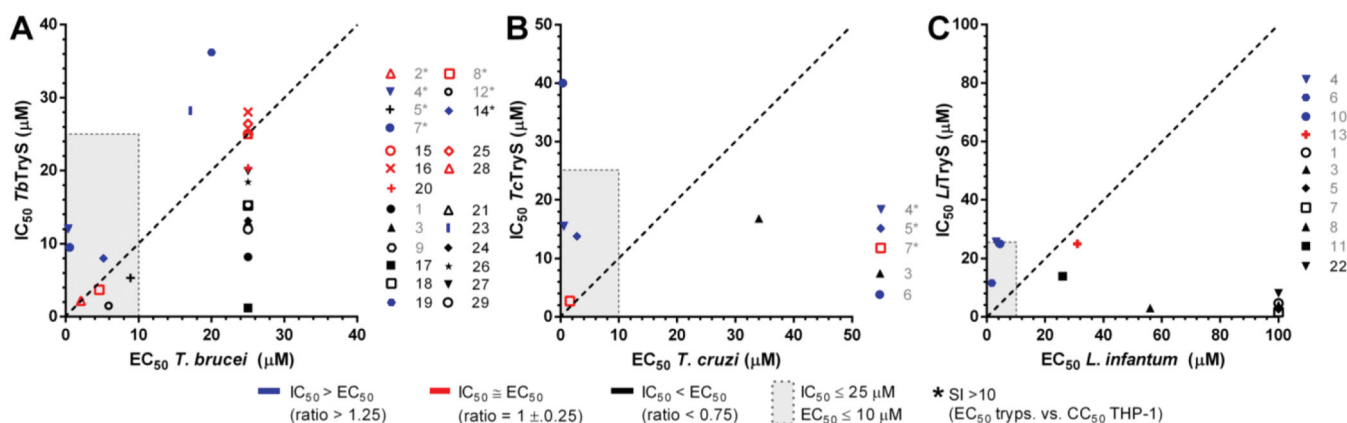


Figure 5. Correlation between on-target (*in vitro*) and anti-trypanosomatid (*in vivo*) activity for selected TryS hits. For the most potent inhibitors of TryS from different trypanosomatid species, the IC_{50} and EC_{50} values are plotted. Compounds showing different correlations for the quotient IC_{50}/EC_{50} are shown in different colours (blue: $IC_{50} > EC_{50}$, red: $IC_{50} \approx EC_{50}$ and black: $IC_{50} < EC_{50}$). The dashed line denotes a correlation for $IC_{50}/EC_{50} = 1$. Compounds inside the grey box are hits against the corresponding TryS ($IC_{50} \leq 25 \mu$ M) and parasite species ($EC_{50} \leq 10 \mu$ M). Those hits that, in addition, present a selectivity index > 10 are highlighted with * in the plot's legend. The results are shown for (A) *Trypanosoma brucei* TryS and bloodstream parasites, (B) *Trypanosoma cruzi* TryS and amastigote stage and (C) *Leishmania infantum* TryS and amastigote stage.

Inhibition of TbTryS by Ebselen was observed as long as the compound (5 μ M) was pre-incubated for 1 h with the enzyme prior to assaying its activity (sample A; Table 3), which is suggestive of a slow-binding inhibition mechanism. A pre-incubation of Ebselen

with the substrates (sample B), including the thiol-containing molecule glutathione, has not impact on enzyme activity (0% TryS inhibition) and, hence, rules out the possibility of a covalent complex between glutathione and Ebselen acting as enzyme inhibitor.

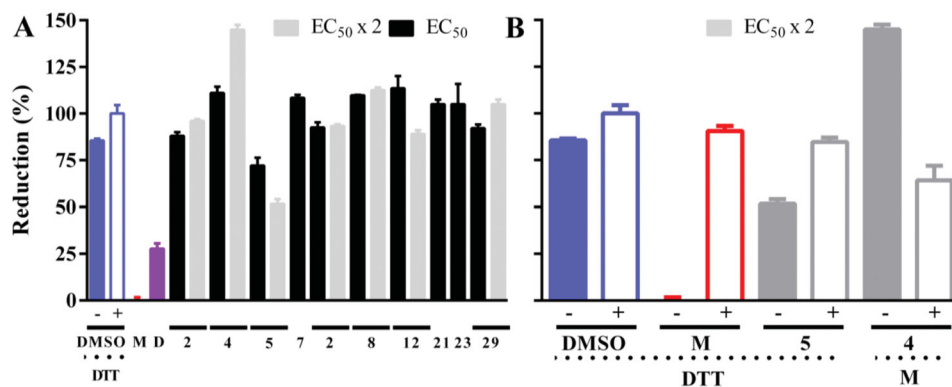


Figure 6. Intracellular redox status of bloodstream *T. b. brucei* treated with TryS's inhibitors. (A) The bloodstream form of a redox reporter cell line of *T. brucei* was treated for 4 h with the most potent compounds targeting TryS and *T. brucei* added at concentrations corresponding to $1\times$ or $2\times$ their EC_{50} (Table 2). The thiol-specific oxidant Diamide (D, $250\ \mu\text{M}$ for 20 min) was included as control. (B) Samples treated with compounds exerting significant changes in biosensor fluorescence, namely 4 and 5 both at $2\times EC_{50}$, were treated for 20 min with menadione (M, $250\ \mu\text{M}$) and DTT (1 mM) to confirm the redox basis of changes observed, respectively. In both plots, the values corresponding to the % reduction of the biosensor are normalised against conditions yielding full biosensor reduction (DTT 1 mM, 20 min) and oxidation (menadione $250\ \mu\text{M}$ for 20 min) in parasites grown in medium containing DMSO 1% v/v.

Table 3. Mode of inhibition of *TbTryS* by Ebselen.

| Time-dependent inhibition assay ^a | Sample | | |
|--|---|----------------|------------------------------|
| | A | B | C |
| Pre-incubation (1 h) | Ebselen + <i>TbTryS</i> | Ebselen + MM | No |
| Reaction (1 h) started with | MM | <i>TbTryS</i> | Ebselen + <i>TbTryS</i> + MM |
| TryS inhibition \pm SD (% , $n = 6$) | 43.6 ± 4.5 | -0.7 ± 2.4 | 1.8 ± 4.2 |
| Irreversible inhibition assay ^b | | | |
| Pre-incubation Ebselen + <i>TbTryS</i> (1 h) | Yes | Yes | Yes |
| Buffer exchanged | Yes | Yes | No |
| Incubation with DTT (5 mM, 30 min) | Yes | No | No |
| TryS inhibition \pm SD (% , $n = 6$) | 89 ± 8.5 | 97.0 ± 5.0 | 100 ± 9 |
| Mass spectrometry analysis ^c | | | |
| 1. Pre-incubation with Ebselen (1 h) | Yes | No | No |
| 2. Pre-incubation IAM ^d (15 mM, 1 h) | No | Yes | No |
| 3. Desalting and IAM ^d treatment (15 mM, 1 h) | Yes | Yes | No |
| TryS inhibition \pm SD (% , $n = 8$) | 100 ± 7 (96 ± 8) ^e | 20 ± 9 | |

TryS activity data (% inhibition) here reported was determined according to the assay described in section *Inhibition mode of candidate hits against TbTryS*.

^aEbselen tested at its IC_{50} against *TbTryS* ($5\ \mu\text{M}$), MM: master mix.

^bEbselen added at two-fold its IC_{50} against *TbTryS* ($10\ \mu\text{M}$).

^cThe data reported correspond to two independent experiments.

^dIAM, iodoacetamide.

^eEbselen added at 4- ($20\ \mu\text{M}$) or 10-folds ($50\ \mu\text{M}$, value in parenthesis) its IC_{50} against *TbTryS*.

Notably, when the pre-incubation enzyme-inhibitor is omitted (sample C), there is a minor effect of Ebselen on enzyme activity (1.8% inhibition), supporting the slow-binding inhibition mechanism and suggesting that the substrates may induce conformational changes in the enzyme that lower the accessibility to the solvent of the site targeted by Ebselen.

Next, a fraction of a sample corresponding to *TbTryS* incubated with the compound ($10\ \mu\text{M}$) for 1 h was buffer exchanged to remove the excess of inhibitor and further treated or not with an excess DTT to evaluate the reversibility of a potential covalent modification of enzyme's cysteine residues. *TbTryS* remained almost fully inhibited upon removal of the inhibitor (97%) and following treatment with an excess DTT (5 mM, 30 min) only a minor fraction of the enzyme recovered activity (89% *TbTryS* inhibition). Overall, these results point to an irreversible modification of the enzyme by Ebselen that may involve the formation of a thiol-selenide bond.

In order to identify a potential covalent modification of *TbTryS* by Ebselen, samples from inhibitor-treated enzyme (sample A, $>96\%$ TryS inhibition; Table 3) were desalted and, to avoid non-

specific disulphide cross-linking during trypsin digestion, free-thiols alkylated with an excess IAM prior to mass spectrometry analysis. A sample of *TbTryS* untreated with Ebselen (Sample B, Mass spectrometry analysis in Table 3) was used as control. Computational analysis using PatternLab allowed a confident identification of *TbTryS* with a sequence coverage ranging from 88.3% to 95.2%. On average, 643 ± 148 spectra could be assigned to peptides from *TbTryS*, covering all peptides containing cysteine residues. Three tryptic and Cys-containing peptides with a mass increment of $274.985\ \text{Da}$ (which is compatible with the incorporation of a single Ebselen molecule *per* peptide) were detected in *TbTryS* treated with Ebselen (Figure 7(A–C)) but not in the control sample. Given the labile nature of the selenide-sulphide bond, during MS/MS analysis the predominant fragmentation is the loss of Ebselen rendering native ion series. Thus, not always was possible to confidently identify the Ebselen-modified residue. However, the detection of the Ebselen modification reporter ions (an intense signal of $m/z = 275.9938$ corresponding to protonated Ebselen plus 2 signals of its most intense fragmentation product of $m/z = 196.0751$ and 183.9417) confirmed the presence of the

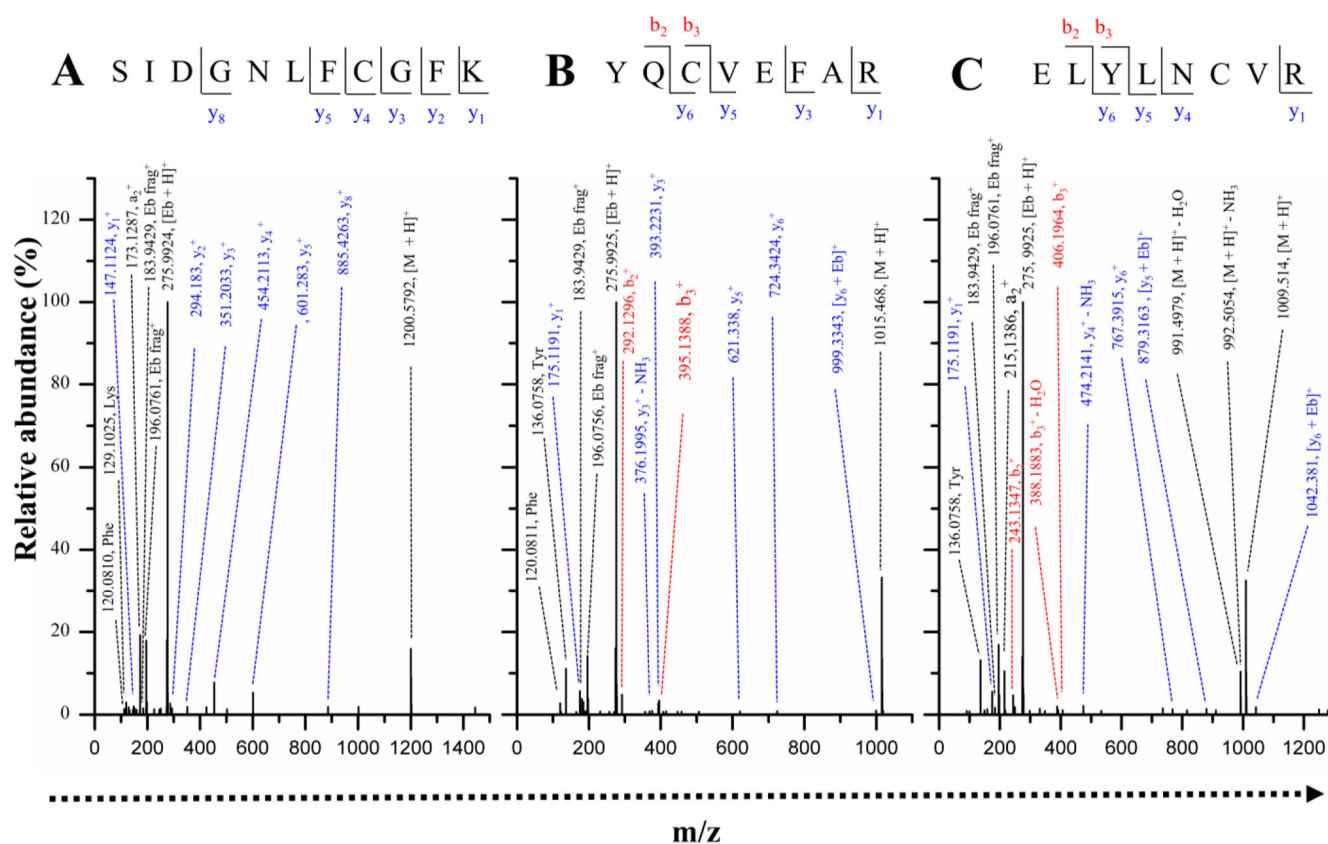


Figure 7. MS/MS spectra of peptides modified by Ebselen. Representative MS/MS spectra for the 3 peptide sequences covalently modified by Ebselen (A) SIDGNLFCGFK ($m/z = 738.2831$, $z = 2$), (B) YQCVEFAR ($m/z = 645.7306$, $z = 2$) and (C) ELYLNCVR ($m/z = 642.7532$, $z = 2$). The Ebselen modification reporter ions (an intense signal of $m/z = 275.9938$ corresponding to protonated Ebselen ($\text{Eb} + \text{H}^+$) and the signal of the two most intense fragmentation products of $m/z = 196.0751$ and 183.9417) are present in all spectra (Eb frag^+). Peaks are assigned to the y and b series of native sequence; +Eb indicates those fragment ions containing the +274.985 modification. Phe, Lys and Tyr indicate the immonium ions of the respective amino acids. Eb: Ebselen.

inhibitor molecule in the peptides of interest. Two of the peptides belong to the papain-like amidase domain (peptide sequences: $\text{S}^{44}\text{IDGNLFCGFK}^{54}$ and $\text{Y}^{55}\text{QCVEFAR}^{62}$) (Figure 7(A,B)) where Cys^{51} is located close to the catalytic site and Cys^{57} along with His^{128} form the catalytic dyad that hydrolyses the C–N bonds of Gsp and T(SH)₂ (Figure 7(A)). Cys^{57} is strictly conserved in Tri-Tryp TryS (Figure 7(A)) whereas Cys^{51} is replaced by a phenylalanine residue in the leishmanial homologue. Although the modification of these cysteines will impair the hydrolytic activity of TryS, it is very unlikely that it will affect the synthetase activity. Therefore, the modification of these peptides has been dismissed as effector of TryS inhibition by Ebselen. The third peptide modified by Ebselen belongs to the synthetase domain (peptide sequence: $\text{E}^{265}\text{LYLNCVR}^{272}$) (Figure 7(C)) and is located at the interphase between the amidase and synthetase domain in a region accessible to the solvent (Figure 8(A,B)).

Interestingly, although the sequence of this peptide varies among Tri-Tryp TryS, its cysteine residue (Cys^{270}) is strictly conserved. Cys^{270} is far from the synthetase active site but is embedded in a highly hydrophobic region formed by three strictly conserved, and consecutive, phenylalanine residues (Phe^{323} , Phe^{325} and Phe^{327}) (Figure 8(A,C)). Such hydrophobic pocket likely favours the anchoring and stabilisation of the Ebselen's benzyl rings. The β -strand containing these residues (β -20) appears to be tightly packed along with the contiguous β -21, both shaping the ATP-binding site (Asp^{331} and Phe^{344} , respectively) and harbouring amino acids that place substrate's reactive groups in the right orientation and proximity of the nucleophilic facilitator residue Ser^{352} (i.e. Arg^{329} and Asn^{347} are hydrogen bonded to γ -phosphate

of ATP and glycyl carboxylate of GSH) (Figure 8(D)). Thus, it is tempting to speculate that Ebselen binding to Cys^{270} has a negative allosteric effect on enzyme active site by destabilising the conformation of strand β -20 (and the vicinal bonds network with strand β -21) and, consequently, by disrupting interactions that might be critical for orienting the substrates in catalytically active conformations.

Mode of inhibition of TbTryS by 17

The mode of TryS inhibition was also investigated for **17**, which represented the most potent and selective singleton from the ENAMINE library targeting the *T. brucei* enzyme. At variance with Ebselen, *TbTryS* inhibition by **17** did not require a pre-incubation of the enzyme with the inhibitor in the absence of substrates (not shown).

Kinetic analysis revealed a complex and substrate-dependent behaviour for the inhibitor. When ATP was the varying substrate, increasing inhibitor concentrations correlated with an increase in enzyme's V_{max} and K_M that rendered a parallel pattern of the double reciprocal substrate versus velocity plots (Figure 9(A)). This behaviour is typical of an uncompetitive inhibition and indicates that the inhibitor does not interfere with ATP binding but, instead, formation of the *TbTryS*-ATP complex favours the interaction with (inhibition by) **17**. For GSH as varying substrate, the Lineweaver-Burk plots were fitted to an exponential equation ($R^2 \geq 0.98$) because inhibition by substrate is observed at $>250 \mu\text{M}$ GSH (Figure 9(B)). The plots' pattern shows dependency on GSH concentration, with converging curves at low GSH concentrations

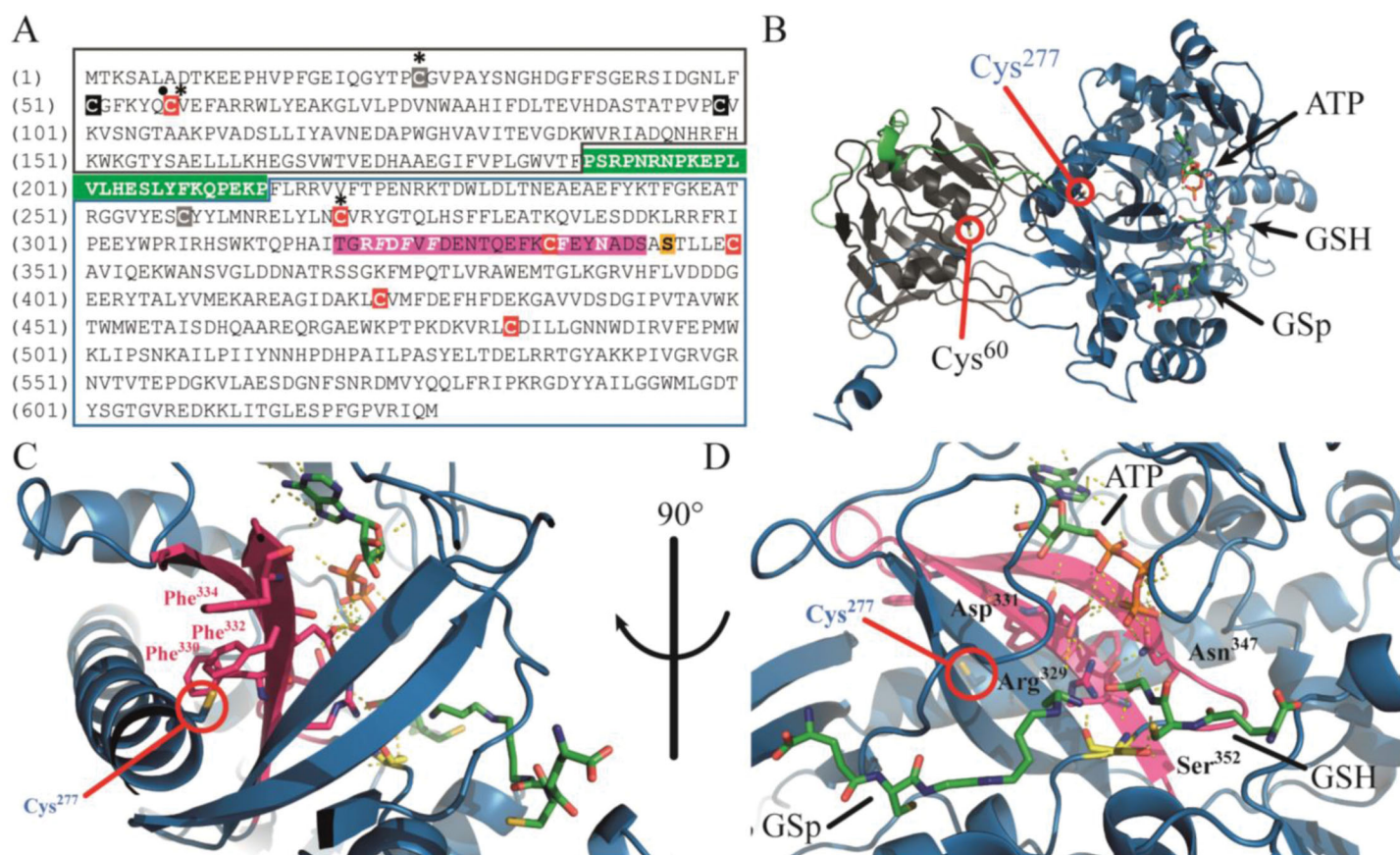


Figure 8. Molecular model for allosteric inhibition of TryS by Ebselen. (A) Amino acid sequence of *Tb*TryS highlighting the N-terminal amidase domain (black box), the C-terminal synthetase domain (blue box) and the linker region (white bold letters on green background). The cysteine residues (red background: conserved in *Tc*- and *Li*-TryS, black background: conserved in *Tc*TryS, grey background: unique to *Tb*TryS) that were found modified by Ebselen (asterisk) and fulfils a role in amidase catalytic activity (dot) are highlighted. The region harbouring structural elements with highly-conserved residues (in white bold letters) relevant for the catalytic activity of the synthetase domain and forming a hydrophobic pocket (italics) in the vicinity of Cys277 is highlighted in magenta background. The strictly conserved serine residue acting as nucleophilic attack facilitator for conjugation of the polyamine moiety (SP or Gsp) to GSH is shown in yellow background. (B) Cartoon representation of *L. major* TryS 3D structure (PDB 2VOB) showing the conserved cysteine residues from the amidase (grey cartoon, Cys60) and the synthetase (blue cartoon, Cys277) domain that bind Ebselen covalently in *Tb*TryS. The linker region is shown in green and the substrates bound to the synthetase active site are shown in sticks. (C) Location of the cysteine from the synthetase domain modified by Ebselen (Cys 277 in *Li*TryS and Cys270 in *Tb*TryS). Hydrophobic residues (Phe330, Phe332 and Phe334) in the vicinity of Cys277 and forming part of structural elements harbouring several residues relevant for catalytic activity are coloured magenta. (D) Synthetase active site with bound substrates and strictly conserved residues relevant for catalysis are shown in magenta (Arg329, Asp331 and Asn347) and yellow (Ser352) coloured sticks. The network of hydrogen bonds and electrostatic interactions between these residues and with substrates is shown with dashed lines.

(<33 μ M) and parallel curves at high GSH concentrations (>33 μ M). This behaviour suggests that **17** does not compete with GSH but exert an allosteric inhibition of TryS (see Equations for substrate inhibition in Supplemental material). With respect to SP, the reciprocal plots displayed a non-linear and parallel pattern, which is compatible with an uncompetitive inhibition of *Tb*TryS (Figure 9(C)). Due to the low K_M value of *Tb*TryS for Gsp (\sim 2.4 μ M)³³, and the low sensitivity of the method used to monitor enzyme activity (Figure S1), it was not possible to perform reactions at sub- K_M concentrations of this substrate. Thus, enzyme inhibition was tested at a single and saturating concentration of Gsp (100 μ M) and the inhibition profile compared to that obtained for SP, also tested at a saturating concentration (4.5 mM). As shown in Figure 9(D), **17** exerts a similar exponential decay in *Tb*TryS activity under saturating concentrations of both polyamine substrates. However, the lower degree of *Tb*TryS inhibition achieved by **17** in the presence of Gsp suggests that the last displaces the inhibitor from the polyamine binding-site better than SP.

Discussion

For its multiple and essential roles in parasite biology and drug resistance, the trypanothione-dependent metabolism of trypanosomatids has attracted attention for the development of specific and effective drugs against these pathogens^{43–45}.

Although TryS proved druggable, the identification and design of inhibitors is challenging due to some peculiar structural and mechanistic features of this enzyme. TryS' active site accommodates four substrates and contains several regions involved in substrate binding that are highly dynamic^{46,47}. During catalysis, the protein adopts different conformations and establishes kinetic complexes with substrates and their intermediate reactants⁴⁸. Such conformational plasticity give rise to large variations in the substrates K_M values among TryS and may explain the reported species-specific inhibition by compounds²⁵. Except for Gsp, the other substrates of TryS (i.e. GSH, ATP and SP) are ubiquitous to and found at high intracellular concentrations in the parasite and host. Thus, the identification of non-competitive inhibitors is highly desirable to overcome competition by a high physiological

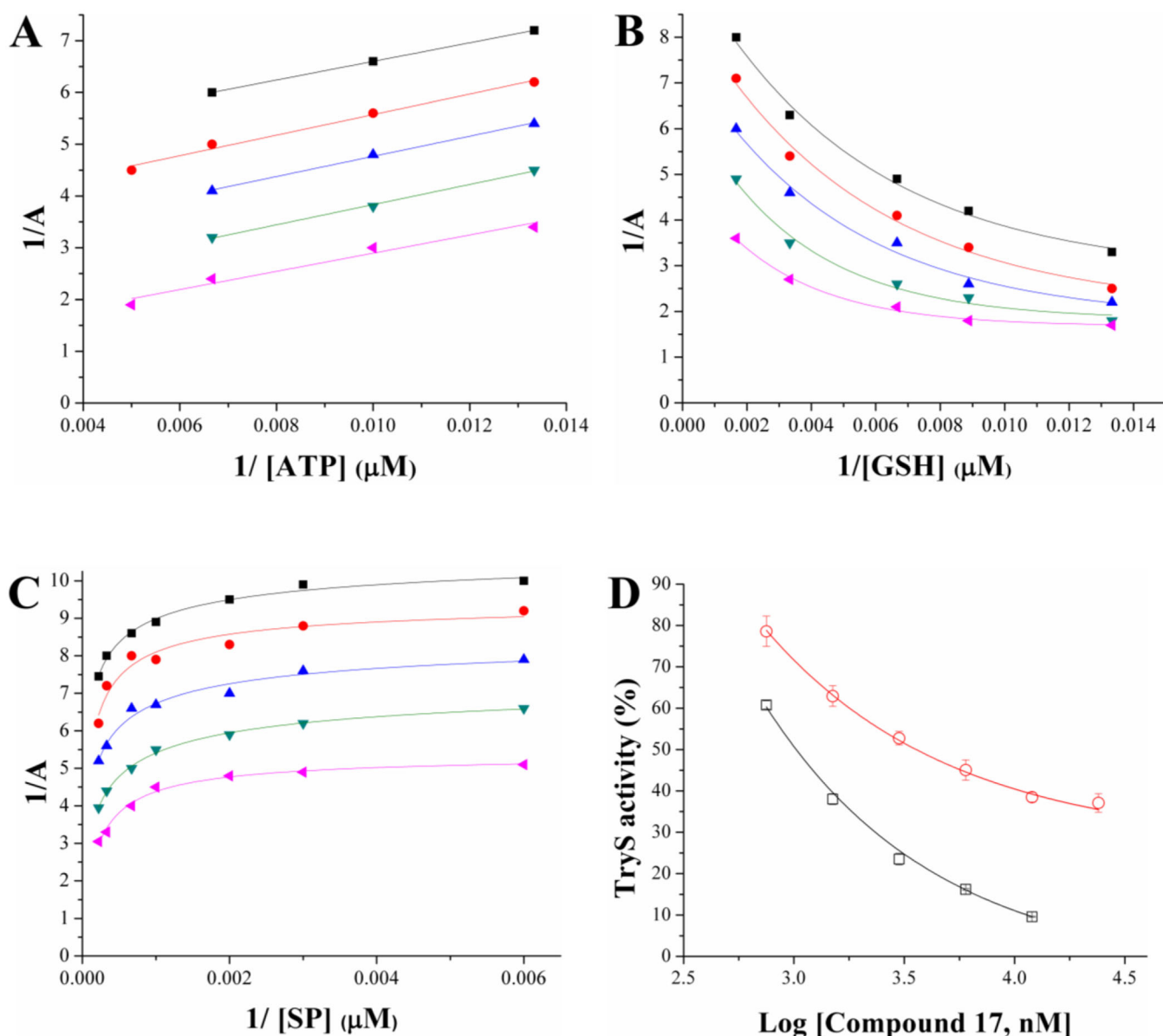


Figure 9. Inhibition mechanism of 17 towards *TbTryS*. Lineweaver–Burk plots are shown for the varying substrate: (A) ATP, (B) glutathione (GSH) and (C) spermidine (SP). The kinetic analysis was performed at different inhibitors (black square: 12 μM , red circle: 6 μM , blue triangle: 3 μM , green inverted triangle: 1.5 μM , and pink triangle: 0.75 μM) and single substrate concentrations while maintaining fixed the concentration of the co-substrates (4.5 mM for SP, 200 μM for ATP and 150 μM for GSH). Enzyme velocity was measured using an end-point assay (see the section 1.3 *Materials and methods* for details). (D) *TbTryS* activity determined at different inhibitor concentrations and saturating concentrations of all substrates (SP: black empty square and Gsp: red empty circle).

concentration of substrates and to avoid potential off-target effects. Our screening assay was performed at near-physiological concentrations ($\geq K_M$ values) of substrates and, hence, highly biased towards the detection of non-competitive or high-affinity competitive ligands. This is in line with the low hit ratio against the molecular target of our screening approach (0.05%) and the good correlation between *in vitro* *TbTryS* inhibition (IC_{50} 1–36 μM) and the selective anti-proliferative activity against bloodstream *T. brucei* (EC_{50} 5–25 μM , seven hits with $\text{SI} > 10$). In contrast, a previous screening campaign against *TbTryS* conducted at sub- K_M concentrations of SP (25 μM) and GSH (20 μM) reported a 24-fold higher hit ratio (1.14%), albeit the hits displayed a 10- to 100-fold lower biological activity (i.e. $\text{IC}_{50} \ll \text{EC}_{50}$)¹². Although several biological arguments were raised by the authors to explain this difference, the more reasonable explanation is that compounds'

potency towards TryS was overestimated under sub- K_M assay conditions.

Most of the broad spectrum TryS inhibitors here identified belong to a library containing molecules with known biochemical and physiological activities, although not all of them with desirable properties as drug candidates. For instance, 6-hydroxy-DL-DOPA (**3**) is a precursor of the catecholaminergic neurotoxin 6-hydroxydopamine used as drug model to induce neurotoxicity in animal models⁴⁹. 6-Hydroxy-DL-DOPA has been reported as an allosteric inhibitor of proteins involved DNA repair (APE1 and RAD52) by interfering with the formation of protein complexes^{50,51}. TryS are monomeric enzymes and structurally unrelated to APE1 and RAD52, moreover 6-hydroxy-DL-DOPA lacks structural similarity with any of the TryS' substrates. Thus, the remarkable capacity of the compound to target Tri-Tryp TryS

suggests a common binding mode, likely at an allosteric site, which deserves further investigation. In this respect and given the lack of pharmacological profile of 6-hydroxy-DL-DOPA and its weak anti-trypanosomatid activity, this scaffold may nevertheless serve as building block for a fragment-based design of multi-species TryS inhibitors.

NH125 (**4**) is an imidazolium *N*-alkylated derivative and a non-specific colloidal aggregator that, as such, inhibits non-specifically and only *in vitro* different kinases (eukaryotic elongation factor 2 (eEF-2) kinase, protein kinase A and C, histidine kinases)⁵². Therefore, this compound can be disregarded as a true active site inhibitor and its potent anti-trypanosomatid activity is likely associated to its capacity to disrupt cell membranes in a detergent-like fashion⁵².

Sanguinarine chloride (**6**) is a polycyclic alkaloid from plants with broad spectrum microbial and cytotoxic activity by targeting multiple molecules and processes⁵³. In eukaryotic cells, it induces an early apoptotic response linked to a substantial depletion of intracellular GSH⁵⁴. Although the compound has no prospect for further clinical applications, biochemically guided molecular down-sizing may open the possibility for the development of TryS inhibitors with improved biological activity and selectivity.

Calmidazolium chloride (**7**) is a positively charged and hydrophobic molecule that has been suggested to exert its biological effect by destabilising membrane phospholipids⁵⁵ rather than by being a calmodulin antagonist⁵⁶. This compound was one of the most potent and selective anti-*Trypanosoma* molecule identified in the biological screening. Interestingly, trypanosomal calmodulin has been shown less sensitive than its vertebrate homologue to inhibition by calmidazolium⁵⁷, which all together suggests that calmidazolium has a different molecular target in the pathogens.

Ebselen (**5**) is an organoselenium compound reported as cysteine oxidant or modifier^{58–60} that inhibits Tri-Tryp TryS within a narrow range of concentrations (IC₅₀ = 3–14 μM). Despite Ebselen may show some promiscuity for modifying thiol groups, not all cysteine residues are capable to react and generate stable complexes with it. This is largely determined by solvent accessibility, polarity of the surrounding medium/residues and thiol pKa. In fact, 6 out of 10 cysteine residues conserved among TryS are accessible to the solvent, likely a few of them deprotonated (to favour the nucleophilic attack on the β-lactam group of Ebselen) and immersed in a non-polar environment to facilitate interactions with the aromatic rings of the ligand. Such criteria were apparently met by two residues from the amidase active site (Cys⁵¹ and Cys⁵⁷) and one from the synthetase domain (Cys²⁷⁰), as suggested by mass spectrometry analysis of Ebselen-Cys protein covalent complexes. Cys²⁷⁰ is at the N-terminus of the longest and highly conserved α-helix (26-residues long; His²⁷¹-Glu²⁹⁷ in *LtTryS*) of TryS. In this position, thiol deprotonation of Cys²⁷⁰ is favoured by the α-helix dipole moment. Although helix α5 is not part of the synthetase active site, it likely serves as structural scaffold for stabilising the nearby strands β-20 and β-21 that shape the nucleotide binding site. It is then tempting to speculate that the incorporation of a bulky Ebselen moiety in helix α5 will exert a conformational change on the vicinal β-20 and -21 leading to the allosteric inhibition of the enzyme. Supporting this hypothesis, alkylation of cysteines residues with the small molecule iodoacetamide had negligible effects on TryS activity. Worth noting, Cys²⁷⁰ as well as other residues and structural elements targeted by this inhibition mechanism are highly conserved in TryS, which agrees with the wide-spectrum inhibitory activity of Ebselen towards Tri-Tryp TryS.

Ebselen was the only hit for which there was a clear correlation between anti-trypanosomal activity and on-target effect in *T. brucei* (intracellular oxidative milieu). This compound has been shown to inhibit trypanothione reductase by covalent formation of seleno-sulphide bonds with enzyme's cysteines⁶⁰. Thus, the strong oxidant effect exerted by Ebselen against bloodstream *T. brucei* is likely consequence of the simultaneous inhibition of two major enzymes from the parasite thiol-redox metabolism: trypanothione reductase and TryS. Ebselen represents an interesting multi-target compound (the essential Cys³²⁷ from *T. brucei* hexokinase has also been shown to be irreversibly oxidised and inactivated by Ebselen)^{61,62} that has been explored in different clinical trials including acute ischaemic stroke⁶³, bipolar disorders in substitution of lithium-therapy^{64,65} and prevention of noise-induced hearing loss⁶⁶. The promiscuity of Ebselen to react with cysteine residues may hamper its clinical efficacy (i.e. sequestration by the cysteine residue from the abundant serum albumin) and repositioning. However, our findings open the possibility for designing new derivatives with improved target selectivity.

Notably, and with the exception of 6-hydroxy-DL-DOPA, a common feature of the multi-TrypS inhibitors described above is their remarkable hydrophobic nature, which suggests the presence of druggable hydrophobic pockets in the enzyme.

In contrast to the *pan*-inhibitory activity of the hits from the *in-house* library, screening of the *ENAMINE* library yielded inhibitors (scaffolds and singletons) highly specific for *TbTryS*. Among them, the AMTPH scaffold shares a common pharmacophore structure (with two hydrogen bond atoms in a 1.5 relationship and one of them located in the thiazole ring) with the phenyl thiazole-based compounds (Figure 1) previously identified as *TbTryS* hits¹². Similar to the hits from the *in-house* library, compound's aromaticity seems to be an important determinant of activity that is conserved in the scaffolds CPA, AMTPH and AMPH, as well as in several singletons. As example, analogues of **17** (potent inhibitor of *TbTryS*) devoid of the adamantane moiety were inactive against *TbTryS*. Lipophilic substitutions in non-competitive, albeit structurally unrelated, TryS hits also proved relevant for inhibitory activity²⁴. Worth noting, both scaffolds consist of a central heterocyclic ring (thiazole for AMTPH and piperidine for CPA) that links aromatic rings of different chemical nature. For the CPA analogues, the aromatic moieties are linked to the heterocycle by acetamide bonds, which suggest that both substituents may freely adopt different spatial conformations. A similar flexibility is expected for one of the substituents of the AMTPH analogues whereas the benzene ring of the second substituent may adopt a planar orientation with the thiazole ring. Probably, this conformational flexibility favour accommodation into the enzyme active site that is structurally complex³⁵.

Our biological data also show an overall higher selectivity index towards *T. brucei* for the hits from the *in-house* library than for those from the *ENAMINE* library, and highlights the difficulties in identifying bioactive and selective compounds acting on the intracellular form of pathogenic trypanosomatids (e.g. *T. cruzi* and *L. infantum*). Differences in the proteome of the infective stage of trypanosomatid species and/or in the molecular targets of the hits may in part account for the low attrition rate. On the other hand, compound metabolism, sequestration, efflux or modification by the host cell are additional factors that may affect the bioactivity against intracellular pathogens and represent major challenges for drug development. Worth noting, at least three hits (**4**, **5** and **7**) showed a killing potency against *T. cruzi* amastigotes in the same order of magnitude than that of the clinical drug benznidazole. Although several hits from the *in-house* library were active against

L. donovani amastigotes, selectivity was highly compromised. *Leishmania* amastigotes reside in the parasitophorous vacuole of macrophages, a hybrid compartment derived from the host endocytic- and containing elements from the secretory-pathway⁶⁷. In addition, to its extreme low pH (4.7–5.3)⁶⁸, the parasitophorous vacuole contains several hydrolytic, proteolytic and efflux activities that may eventually reduce compounds bioavailability and activity. Importantly, our study identified seven new biological hits against bloodstream *T. brucei*.

Our drug discovery campaign disclosed new chemical structures targeting a key enzyme of the parasite redox metabolism and the infective stage of pathogenic trypanosomatids. The hits represent good candidates to undertake optimisation strategies aimed to enhance their inhibitory activity against TryS and pharmacological properties. Last but not least, the full set of data (positive and negative results) collected in the TryS-screening deems valuable for feeding artificial intelligence drug discovery approaches⁶⁹, which have the potential for screening larger virtual chemolibraries (including drug repositioning libraries).

Acknowledgements

The authors thank Dr Alan Fairlamb (Dundee University, Scotland) for providing expression plasmid for TryS from *T. brucei*. D. B. acknowledges Dr Hyu Ho Paul Park (Dengue Research Laboratory, Institut Pasteur Korea, South Korea) for assistance during protein purification. The authors thank Fanny Lenglard (Université de Caen Normandie, France) for her assistance to FS during her short-internship at Institut Pasteur of Montevideo. DB thanks Institut Pasteur Korea staff, in particular its former Chief Executive Officer Dr Hakim Djballah, for his kind help during D. B.'s internship in South Korea.

Disclosure statement

The authors report no conflict of interest.

Funding

This work was supported by the "Le Réseau International des Instituts Pasteur (RIIP)", "Actions Concertées Internationales Pasteuriennes" [Grant nos. 17–2015]; and FOCEM (Fondo para la Convergencia Estructural del Mercosur) [Grant no. COF 03/11].

References

1. WHO. Research priorities for Chagas disease, Human African Trypanosomiasis and Leishmaniasis. Technical report of the TDR disease reference group on Chagas disease, Human African Trypanosomiasis and Leishmaniasis. Technical Report 2012. <https://apps.who.int/iris/handle/10665/77472>
2. Comini MA, Flohé L. The trypanothione-based redox metabolism of trypanosomatids. In: T Jäger, O Koch, L Flohé, eds. Trypanosomatids diseases: molecular routes to drug discovery (drug discovery in infectious diseases). Oxford: Wiley-Blackwell; 2013:167–199.
3. Anantharaman V, Aravind L. Evolutionary history, structural features and biochemical diversity of the NlpC/P60 superfamily of enzymes. *Genome Biol* 2003;4:R11.
4. Fawaz MV, Topper ME, Firestone SM. The ATP-grasp enzymes. *Bioorg Chem* 2011;39:185–91.
5. Comini MA, Biosynthesis of polyamine–glutathione derivatives in Enterobacteria and Kinetoplastida. In: L Flohé, ed. Glutathione. London: CRC Press; 2018:285–305.
6. Comini MA, Guerrero SA, Haile S, et al. Validation of *Trypanosoma brucei* trypanothione synthetase as drug target. *Free Radic Biol Med* 2004;36:1289–302.
7. Ariyanayagam MR, Oza SL, Guther ML, Fairlamb AH. Phenotypic analysis of trypanothione synthetase knockdown in the African trypanosome. *Biochem J* 2005;391:425–32.
8. Sousa AF, Gomes-Alves AG, Benítez D, et al. Genetic and chemical analyses reveal that trypanothione synthetase but not glutathionylspermidine synthetase is essential for *Leishmania infantum*. *Free Radic Biol Med* 2014;73:229–38.
9. Mesías AC, Sasoni N, Arias DG, et al. Trypanothione synthetase confers growth, survival advantage and resistance to anti-protozoal drugs in *Trypanosoma cruzi*. *Free Radic Biol Med* 2019;130:23–34.
10. Manta B, Bonilla M, Fiestas L, et al. Polyamine-based thiols in trypanosomatids: evolution, protein structural adaptations, and biological functions. *Antioxid Redox Signal* 2018; 28:463–86.
11. Wyllie S, Oza SL, Patterson S, et al. Dissecting the essentiality of the bifunctional trypanothione synthetase-amidase in *Trypanosoma brucei* using chemical and genetic methods. *Mol Microbiol* 2009;74:529–40.
12. Torrie LS, Wyllie S, Spinks D, et al. Chemical validation of trypanothione synthetase: a potential drug target for human trypanosomiasis. *J Biol Chem* 2009;284:36137–45.
13. Medeiros A, Benítez D, Korn RS, et al. Mechanistic and biological characterisation of novel N5-substituted paullones targeting the biosynthesis of trypanothione in *Leishmania*. *J Enzyme Inhib Med Chem* 2020;35:1345–58.
14. Olin-Sandoval V, González-Chávez Z, Berzunza-Cruz M, et al. Drug target validation of the trypanothione pathway enzymes through metabolic modelling. *Febs J* 2012;279: 1811–33.
15. Chen S, Lin CH, Walsh CT, Coward JK. Novel inhibitors of trypanothione biosynthesis: synthesis and evaluation of a phosphinate analog of glutathionyl spermidine (GSP), a potent, slow binding inhibitor of GSP synthetase. *Bioorg Med Chem Lett* 1997;7:505–10.
16. Chen S, Lin CH, Kwon DS, et al. Design, synthesis, and biochemical evaluation of phosphonate and phosphoramidate analogs of glutathionylspermidine as inhibitors of glutathionylspermidine synthetase/amidase from *Escherichia coli*. *J Med Chem* 1997;40:3842–50.
17. Verbruggen C, De Craecker S, Rajan PK, et al. Phosphonic acid and phosphinic acid tripeptides as inhibitors of glutathionylspermidine synthetase. *Bioorg Med Chem Lett* 1996; 6:253–8.
18. Kwon DS, Lin CH, Chen S, et al. Dissection of glutathionylspermidine synthetase/amidase from *Escherichia coli* into autonomously folding and functional synthetase and amidase domains. *J Biol Chem* 1997;272:2429–36.
19. Lin CH, Chen S, Kwon DS, et al. Aldehyde and phosphinate analogs of glutathione and glutathionylspermidine: potent, selective binding inhibitors of the *E. coli* bifunctional glutathionylspermidine synthetase/amidase. *Chem Biol* 1997;4: 859–66.
20. Amssoms K, Oza SL, Ravaschino E, et al. Glutathione-like tripeptides as inhibitors of glutathionylspermidine synthetase. Part 1: substitution of the glycine carboxylic acid group. *Bioorg Med Chem Lett* 2002;12:2553–6.

21. Amsoms K, Oza SL, Augustyns K, et al. Glutathione-like tripeptides as inhibitors of glutathionylspermidine synthetase. Part 2: substitution of the glycine part. *Bioorg Med Chem Lett* 2002;12:2703–5.
22. Oza SL, Chen S, Wyllie S, et al. ATP-dependent ligases in trypanothione biosynthesis—kinetics of catalysis and inhibition by phosphinic acid pseudopeptides. *Febs J* 2008;275:5408–21.
23. D’Silva C, Daunes S. Structure-activity study on the in vitro antiprotozoal activity of glutathione derivatives. *J Med Chem* 2000;43:2072–8.
24. Spinks D, Torrie LS, Thompson S, et al. Design, synthesis and biological evaluation of *Trypanosoma brucei* trypanothione synthetase inhibitors. *ChemMedChem* 2012;7:95–106.
25. Benítez D, Medeiros A, Fiestas L, et al. Identification of novel chemical scaffolds inhibiting trypanothione synthetase from pathogenic trypanosomatids. *PLoS Negl Trop Dis* 2016;10:e0004617.
26. Orban OC, Korn RS, Benítez D, et al. 5-Substituted 3-chloro-kenpauillone derivatives are potent inhibitors of *Trypanosoma brucei* bloodstream forms. *Bioorg Med Chem* 2016;24:3790–800.
27. Biebinger S, Wirtz LE, Lorenz P, Clayton C. Vectors for inducible expression of toxic gene products in bloodstream and procyclic *Trypanosoma brucei*. *Mol Biochem Parasitol* 1997;85:99–112.
28. Gutscher M, Pauleau AL, Marty L, et al. Real-time imaging of the intracellular glutathione redox potential. *Nat Methods* 2008;5:553–9.
29. Hirumi H, Hirumi K. Continuous cultivation of *Trypanosoma brucei* blood stream forms in a medium containing a low concentration of serum protein without feeder cell layers. *J Parasitol* 1989;75:985–9.
30. Maiwald F, Benítez D, Charquero D, et al. 9- and 11-Substituted 4-azapauillones are potent and selective inhibitors of *African trypanosoma*. *Eur J Med Chem* 2014;83:274–83.
31. Carvalho PC, Lima DB, Leprevost FV, et al. Integrated analysis of shotgun proteomic data with PatternLab for proteomics 4.0. *Nat Protoc* 2016;11:102–17.
32. Perez-Riverol Y, Csordas A, Bai J, et al. The PRIDE database and related tools and resources in 2019: improving support for quantification data. *Nucleic Acids Res* 2019;47:D442–50.
33. Oza SL, Ariyanayagam MR, Aitcheson N, Fairlamb AH. Properties of trypanothione synthetase from *Trypanosoma brucei*. *Mol Biochem Parasitol* 2003;131:25–33.
34. Zhang JH, Chung TD, Oldenburg KR. A simple statistical parameter for use in evaluation and validation of high throughput screening assays. *J Biomol Screen* 1999;4:67–73.
35. Don R, loset JR. Screening strategies to identify new chemical diversity for drug development to treat kinetoplastid infections. *Parasitology* 2014;141:140–6.
36. Ebersoll S, Bogacz M, Günter LM, et al. A tryparedoxin-coupled biosensor reveals a mitochondrial trypanothione metabolism in trypanosomes. *Elife* 2020;9:e53227.
37. Franco J, Sardi F, Szilágyi L, et al. Diglycosyl diselenides alter redox homeostasis and glucose consumption of infective *African trypanosomes*. *Int J Parasitol Drugs Drug Resist* 2017;7:303–13.
38. Franco J, Medeiros A, Benítez D, et al. In vitro activity and mode of action of distamycin analogues against *African trypanosomes*. *Eur J Med Chem* 2017;126:776–88.
39. Rodríguez Arce E, Putzu E, Lapier M, et al. New heterobimetallic ferrocenyl derivatives are promising antitrypanosomal agents. *Dalton Trans* 2019;48:7644–58.
40. Franco J, Scarone L, Comini MA. Novel distamycin analogues that block the cell cycle of *African trypanosomes* with high selectivity and potency. *Eur J Med Chem* 2020;189:112043.
41. Rivas F, Medeiros A, Quiroga C, et al. New Pd-Fe ferrocenyl antiparasitic compounds with bioactive 8-hydroxyquinoline ligands: a comparative study with their Pt-Fe analogues. *Dalton Trans* 2021;50:1651–65.
42. Ortíz C, Moraca F, Laverriere M, et al. Glucose 6-phosphate dehydrogenase from trypanosomes: selectivity for steroids and chemical validation in bloodstream *Trypanosoma brucei*. *Molecules* 2021;26:358.
43. Franco J, Scarone L, Comini MA. Drugs and drug resistance in African and American Trypanosomiasis. In: M Botta, ed. *Annual reports in medicinal chemistry: neglected diseases: extensive space for modern drug discovery*. New York (NY): Academic Press, Elsevier Inc.; 2018:97–133.
44. Talevi A, Carrillo C, Comini M. The thiol-polyamine metabolism of *Trypanosoma cruzi*: molecular targets and drug repurposing strategies. *Curr Med Chem* 2019;26:6614–35.
45. Saccoliti F, Di Santo R, Costi R. Recent advancement in the search of innovative antiprotozoal agents targeting trypanothione metabolism. *ChemMedChem* 2020;15:2420–35.
46. Fyfe PK, Oza SL, Fairlamb AH, Hunter WN. Leishmania trypanothione synthetase-amidase structure reveals a basis for regulation of conflicting synthetic and hydrolytic activities. *J Biol Chem* 2008;283:17672–80.
47. Koch O, Cappel D, Nocker M, et al. Molecular dynamics reveal binding mode of glutathionylspermidine by trypanothione synthetase. *PLoS One* 2013;8:e56788.
48. Leroux AE, Haanstra JR, Bakker BM, Krauth-Siegel RL. Dissecting the catalytic mechanism of *Trypanosoma brucei* trypanothione synthetase by kinetic analysis and computational modeling. *J Biol Chem* 2013;288:23751–64.
49. Duty S, Jenner P. Animal models of Parkinson’s disease: a source of novel treatments and clues to the cause of the disease. *Br J Pharmacol* 2011;164:1357–91.
50. Simeonov A, Kulkarni A, Dorjsuren D, et al. Identification and characterization of inhibitors of human apurinic/apyrimidinic endonuclease APE1. *PLoS One* 2009;4:e57403rd.
51. Chandramouly G, McDevitt S, Sullivan K, et al. Small-molecule disruption of RAD52 rings as a mechanism for precision medicine in BRCA-deficient cancers. *Chem Biol* 2015;22:1491–504.
52. Devkota AK, Tavares CD, Warthaka M, et al. Investigating the kinetic mechanism of inhibition of elongation factor 2 kinase by NH125: evidence of a common in vitro artifact. *Biochemistry* 2012;51:2100–12.
53. Kim W, Fricke N, Conery AL, et al. NH125 kills methicillin-resistant *Staphylococcus aureus* persists by lipid bilayer disruption. *Future Med Chem* 2016;8:257–69.
54. Vlachojannis C, Magora F, Chrubasik S. Rise and fall of oral health products with Canadian bloodroot extract. *Phytother Res* 2012;26:1423–6.
55. Debiton E, Madelmont JC, Legault J, Barhomeuf C. Sanguinarine-induced apoptosis is associated with an early and severe cellular glutathione depletion. *Cancer Chemother Pharmacol* 2003;51:474–82.
56. Anderson KW, Coll RJ, Murphy AJ. Inhibition of skeletal muscle sarcoplasmic reticulum CaATPase activity by calmidazolium. *J Biol Chem* 1984;259:11487–90.

57. Gietzen K. Comparison of the calmodulin antagonists compound 48/80 and calmidazolium. *Biochem J* 1983;216:611–6.
58. Garcia-Marchan Y, Sojo F, Rodriguez E, et al. *Trypanosoma cruzi* calmodulin: cloning, expression and characterization. *Exp Parasitol* 2009;123:326–33.
59. Terentis AC, Freewan M, Sempértegui Plaza TS, et al. The selenazal drug Ebselen potently inhibits indoleamine 2,3-dioxygenase by targeting enzyme cysteine residues. *Biochemistry* 2010;49:591–600.
60. Lu J, Vodnala SK, Gustavsson AL, et al. Ebsulfur is a benzisothiazolone cytotoxic inhibitor targeting the trypanothione reductase of *Trypanosoma brucei*. *J Biol Chem* 2013;288:27456–68.
61. Joice AC, Harris MT, Kahney EW, et al. Exploring the mode of action of Ebselen in *Trypanosoma brucei* hexokinase inhibition. *Int J Parasitol Drugs Drug Resist* 2013;3:154–60.
62. Sharlow ER, Lyda TA, Dodson HC, et al. A target-based high throughput screen yields *Trypanosoma brucei* hexokinase small molecule inhibitors with antiparasitic activity. *PLoS Negl Trop Dis* 2010;4:e659.
63. Yamaguchi T, Sano K, Takakura K, et al. Ebselen in acute ischemic stroke: a placebo-controlled, double-blind clinical trial. Ebselen study group. *Stroke* 1998;29:12–7.
64. Masaki C, Sharpley AL, Cooper CM, et al. Effects of the potential lithium-mimetic, Ebselen, on impulsivity and emotional processing. *Psychopharmacology (Berl)* 2016;233:2655–61.
65. Singh N, Sharpley AL, Emir UE, et al. Effect of the putative lithium mimetic Ebselen on brain myo-inositol, sleep, and emotional processing in humans. *Neuropsychopharmacology* 2016;41:1768–78.
66. Kil J, Lobarinas E, Spankovich C, et al. Safety and efficacy of Ebselen for the prevention of noise-induced hearing loss: a randomised, double-blind, placebo-controlled, phase 2 trial. *Lancet* 2017;390:969–79.
67. Young J, Kima PE. The *Leishmania parasitophorous* vacuole membrane at the parasite–host interface. *Yale J Biol Med* 2019;92:511–21.
68. Antoine JC, Prina E, Jouanne C, Bongrand P. Parasitophorous vacuoles of *Leishmania amazonensis*-infected macrophages maintain an acidic pH. *Infect Immun* 1990;58:779–87.
69. Alice JI, Bellera CL, Benítez D, et al. Ensemble learning application to discover new trypanothione synthetase inhibitors. *Mol Divers* 2021;25:1361–73.